Synthesis of "Fe^{4+}"-Bearing Compounds under High Oxygen Pressures

by

Shigemitsu SHIN

Faculty of Technology, Tokyo Institute of Technology, Tokyo.

Synthesis of "Fe^{4+}"-Bearing Compounds under High Oxygen Pressures

by Shigemitsu SHIN

Faculty of Technology, Tokyo Institute of Technology, Tokyo.

INDEX

Chapter 1

Introduction

Interest in the perovskite compounds (ABO_3) has been great because their crystal structure stabilizes an abnormal valence state of the B ion more easily than any other compounds. Strontium and barium ferrates with some oxygen deficiency, i.e., $SrFeO_3$ (IV) and $BaFeO_3$ (IV), which has been first prepared by Scholder et al.[1] and Erchak et al.,[2] respectively, are good examples. These compounds contain alkaline-earth ions in the A sites while the B sites are occupied by transition-metal ions. The stability of such an abnormal valence state as Fe^{4+} in these compounds may be ascribable to the perovskite structure in which the octahedral B sites are open to the transition-metal cations.

A stoichiometric strontium ferrate (IV) with the perovskite structure has been prepared recently by MacChesney et al.[3] for the first time when anion-deficient strontium ferrate was annealed at a high oxygen pressure and a rather low temperature. From the experimental result, it has been deduced that a perfectly stoichiometric perovskite phase with iron (IV) could be produced only through intense oxidation because of the higher fourth ionization potential of iron,* while, the unique perovskite structure could make the formation of anion-deficient iron (IV)-

---

* The fourth ionization potential of iron is presented in Fig. A1 in Appendix.

bearing strontium ferrate possible even in air. Similar situation has been known for barium ferrate (IV).[4)-6)]

Non-stoichiometry in oxygen fraction, which being revealed in these alkaline-earth ferrates, may cause the perovskites to exhibit specific characters in crystal structure, magnetism and electricity, resulting from the formation of the "mixed" valence state[7)] of iron. In fact, many experimental data has been accumulated by several authors,[1)-14)] concerning the characteristic properties of strontium and barium ferrates (III, IV).

According to the previous crystallographic investigation, the perovskite phase with the chemical composition, $SrFeO_{3-\delta}$ or $BaFeO_{3-\delta}$ (δ refers to oxygen deficiency) is the presumed isomorph of $SrTiO_3$ or $BaTiO_3$, respectively,[15)] whereas the most anion-deficient compounds with the composition, i.e., $SrFeO_{2.5}$ or $BaFeO_{2.5}$, is no longer a perovskite but has a structure corresponding to that of dicalcium ferrite ($Ca_2Fe_2O_5$).[16)*] Subsequently, it has been proposed that the chemical composition of the systems should be denoted as $AFeO_{3-\delta}$ (A = alkaline-earth metal ion; $0 \leqq \delta \leqq 0.5$).

On the other hand, no iron (IV)-bearing calcium ferrate with the perovskite structure has ever been prepared but dicalcium ferrite ($Ca_2Fe_2O_5$) has been known as a stable form in the system $CaFeO_{2.5-3.0}$ despite of the existence of the analog $CaTiO_3$.

---

* The revised data for the atomic coordinates of $Ca_2Fe_2O_5$ lattice were reported (see Reference 17).

From the historical point of view, the fact that a "genuine" perovskite ($CaTiO_3$) occurs as a natural product which has stimulated the discovery of such dielectric materials as $BaTiO_3$ and $SrTiO_3$ and that the latter two perovskites have in turn encouraged us to prepare the presumed isomorphs, $BaFeO_3$ and $SrFeO_3$, it is also an interesting problem to inquire why $CaFeO_3$ (IV) is difficult to be synthesized, and to investigate the crystallographic description of iron (IV)-bearing alkaline-earth ferrates.

Present paper describes a "high oxygen pressure" effect in the system $(Ca_xSr_{1-x})FeO_{3-\delta}$ ($0 \leqq x \leqq 1$, with x in the steps of 0.2 mole; $0 \lesssim \delta \leqq 0.5$) as well as the characterization of the resulting compounds in the system by their physico-chemical properties based on X-ray diffractometry, ^{57}Fe Mössbauer spectroscopy and the measurements of magnetic susceptibility and electric resistivity (chapter 2). The following chapter refers to the details of the synthesis of a new perovskite $CaFeO_3$. Finally, all of the results obtained in the present studies will be summarized in chapter 4.

Chapter 2

High Oxygen Pressure Effect in the System $(Ca_xSr_{1-x})FeO_{3-\delta}$(III,IV)

In this chapter, the author describes the preparation of Fe^{4+}-bearing perovskites in the system $(Ca_xSr_{1-x})FeO_{3-\delta}$ using a high oxygen gas pressure technique and also the physico-chemical properties of the products.

EXPERIMENTAL PROCEDURES

1) Preparation of samples

Starting materials with the chemical composition $(Ca_xSr_{1-x})FeO_{3-\delta}$($0 < \delta \leqq 0.5$; $0 \leqq x \leqq 1$) were prepared as follows: the calculated amounts of standardized 1 M calcium, strontium and ferric nitrate solutions were mixed. The mixture was transferred into a 250-ml fused silica beaker and evaporated to dryness on a water bath. The dried salts were then heated on a strong fire to decompose any residual nitrates. Next the residue was ground intimately in an agate motar, and then transferred into a platinum crucible in order to be subjected to several times' pre-firings at 600 to 1100°C. Finally the calcined matter was re-ground in an agate motar and then fired at a desired temperature, 1100 or 1200°C for 6 to 24 hrs.

A series of samples with the higher oxygen contents (i.e., higher Fe^{4+}-concentration) was prepared by heating the starting materials at oxygen pressures ranging from 20 up to 1900 atm in a reactor of the design shown in Figs. 1 and 2. A half-sealed

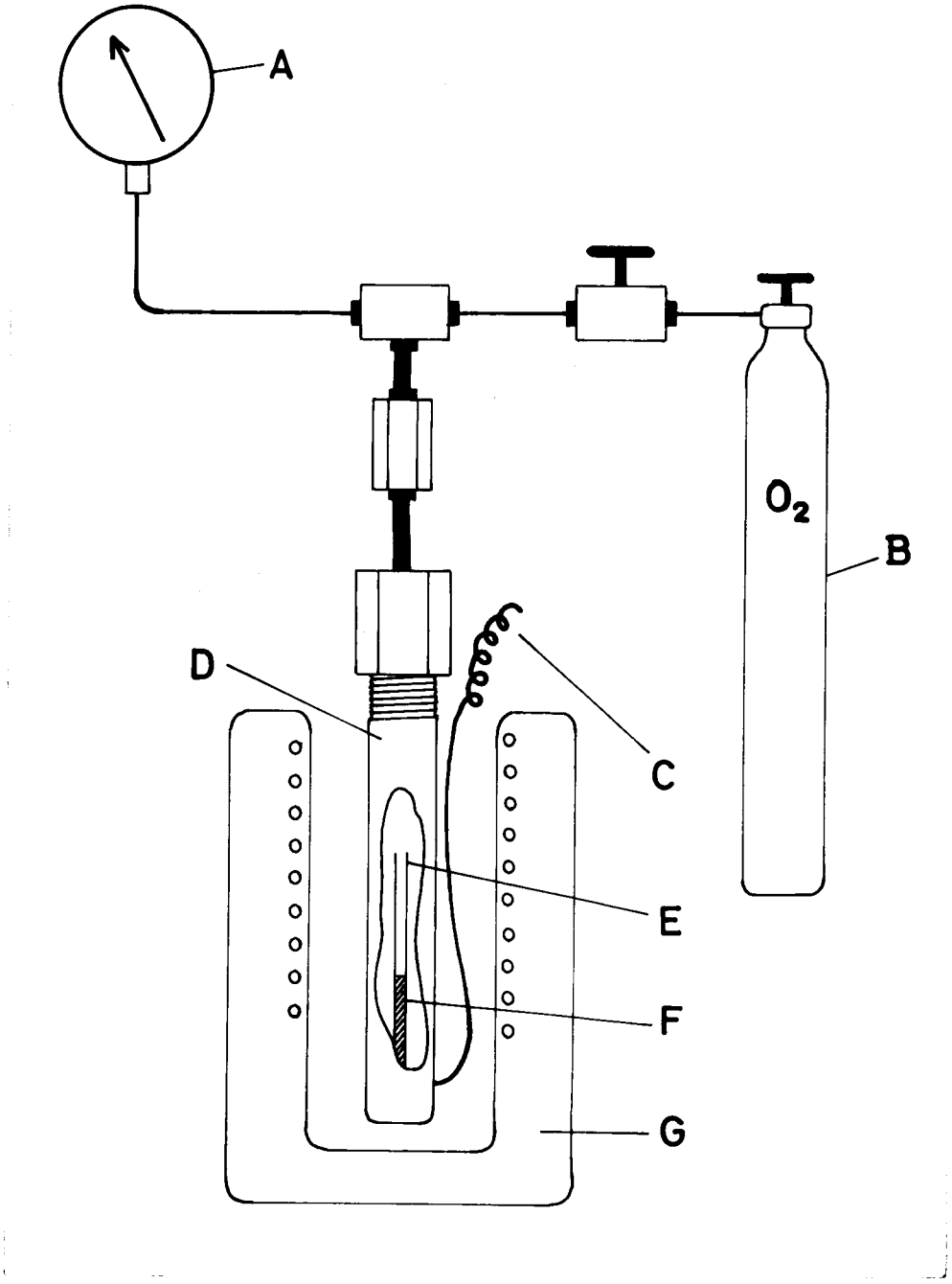

Fig. 1. Apparatus for phase studies at oxygen pressures up to 200 atm consisted of A: Bourdon gauge, B: oxygen reservoir, C: thermocouple leads, D: test-tube-type reactor, E: half-sealed gold tube, F: sample, and G: electric furnace.

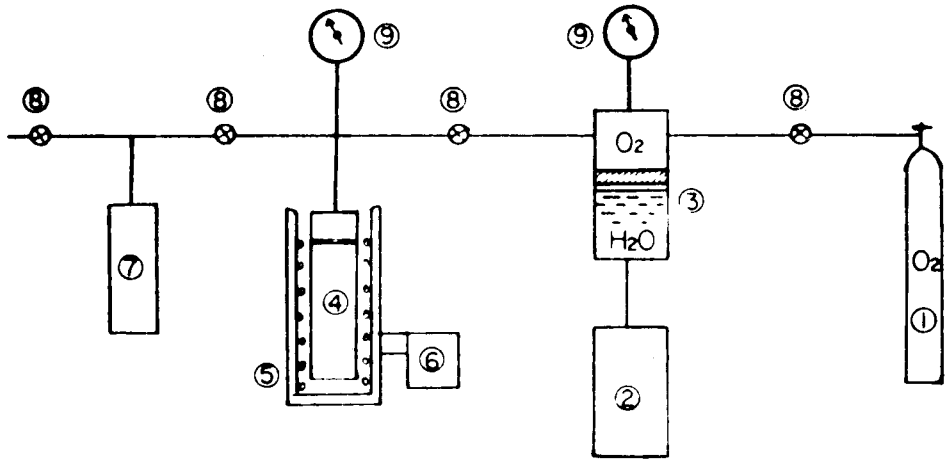

Fig. 2. Apparatus for phase studies at oxygen pressures up to 2000 atm consisted of (1) oxygen reservoir, (2) intensifier, (3) oxygen gas compression cylinder, (4) test-tube-type reactor, (5) electric furnace, (6) temperature-indicating controller, (7) vacuum pump, (8) valves, and (9) pressure gauges.

gold tube was used as a container of the sample in the oxidation procedure. The oxidized sample was cooled with the reactor.

2) Determination of chemical compositions

The oxygen contents in each sample were determined first by a method using both iodometry and a permanganate titration. The iodometry used is a modified method of Guernsey's iodometric titration which he applied for the determination of the Fe^{4+} contents in the system $SrFeO_3$-$SrTiO_3$.[9] The procedure developed in the present analysis is as follows: into a 200-ml Erlenmeyer-flask ca. 350 mg of sample and 10 g of solid potassium iodide were put together with 100 ml of 6 N hydrochloric acid. The specimen was then reacted, with the open end of the flask protected from the atmosphere by a carbon dioxide seal. The liberated iodine was titrated with a 0.1 N standard $Na_2S_2O_3$ solution by using an aliquot of a starch solution as an internal indicator. From the volume of the standard solution required for this titration and the total iron contents determined by a normal permanganate method,[18] the ratio of Fe^{4+}/Fe_{total} was computed in percent.

Thermogravimetric analysis was next applied for the more quantitative determination of the chemical compositions in the system $(Ca_xSr_{1-x})FeO_{3-\delta}$. The author mainly used the δ-values found by this method in the detailed discussion on the relationship between the chemical compositions of the system and their physico-chemical properties. The analytical procedure is as follows: ca. 200 mg of sample was put in a platinum crucible

which was suspended in a tungsten-wound furnace. The sample was then heated slowly in vacuum of 10^{-5} mmHg. One of the TGA curves obtained by this method for the compositions $(Ca_xSr_{1-x})FeO_{3-\delta}$ is shown in Fig. 3. It appears that any weight loss is not found at temperatures above ca. 900°C. An X-ray diffractogram is given for the thermal reaction product in Fig. 4, which implies that this material has a brownmillerite*-like composition ($SrFeO_{2.5}$) in which all of iron ions are reduced in the trivalent state. Therefore, the reaction formula,

$$AFeO_{3-\delta}(III, IV) \xrightarrow[10^{-5}\ mmHg]{>900°C} AFeO_{2.5}(III) + \frac{1-2\delta}{4} O_2,$$

(Initial specimen) (Reduced specimen) (Liberated oxygens)

is given where A denotes Ca and/or Sr atoms. Chemical compositions of the system were obtained from the number of released oxygens.

3) X-ray diffractometry

For the determination of the resulting phase in the system $(Ca_xSr_{1-x})FeO_{3-\delta}$, an X-ray diffractometer (Rigaku Denki Co.Ltd.) was used. Scanning speeds of a goniometer and chart were 2°/min, and 2cm/min, respectively. A slit system of 1°-0.15-1° was used. Copper Kα, CoKα and FeKα radiations were used as an X-ray source. Diffractograms were obtained by employing Geiger-Müller and scintillation counters.

---

* Brownmillerite has a chemical composition of Ca_2AlFeO_5 and a structure similar to that of dicalcium ferrite.[16), 17)]

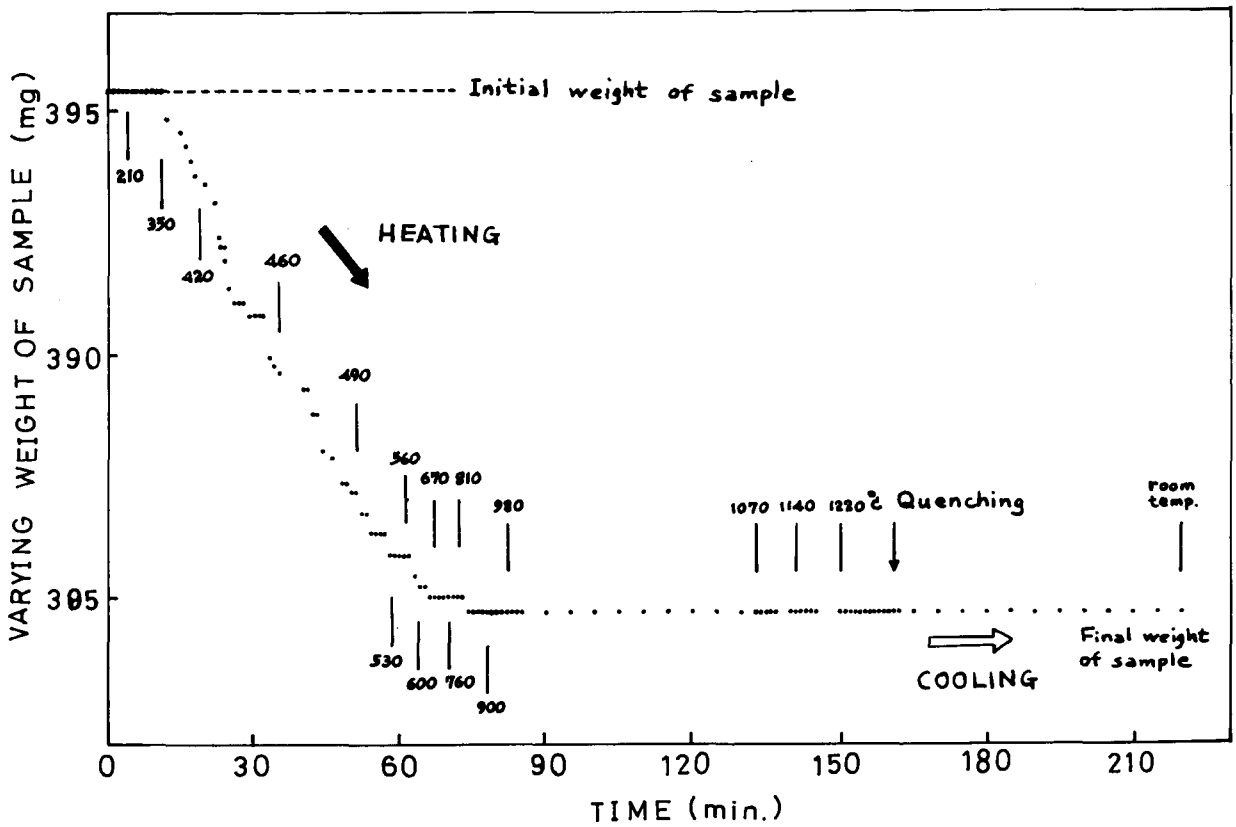

Fig. 3. Thermogravimetric analysis of $SrFeO_{2.81}$ in vacuo.

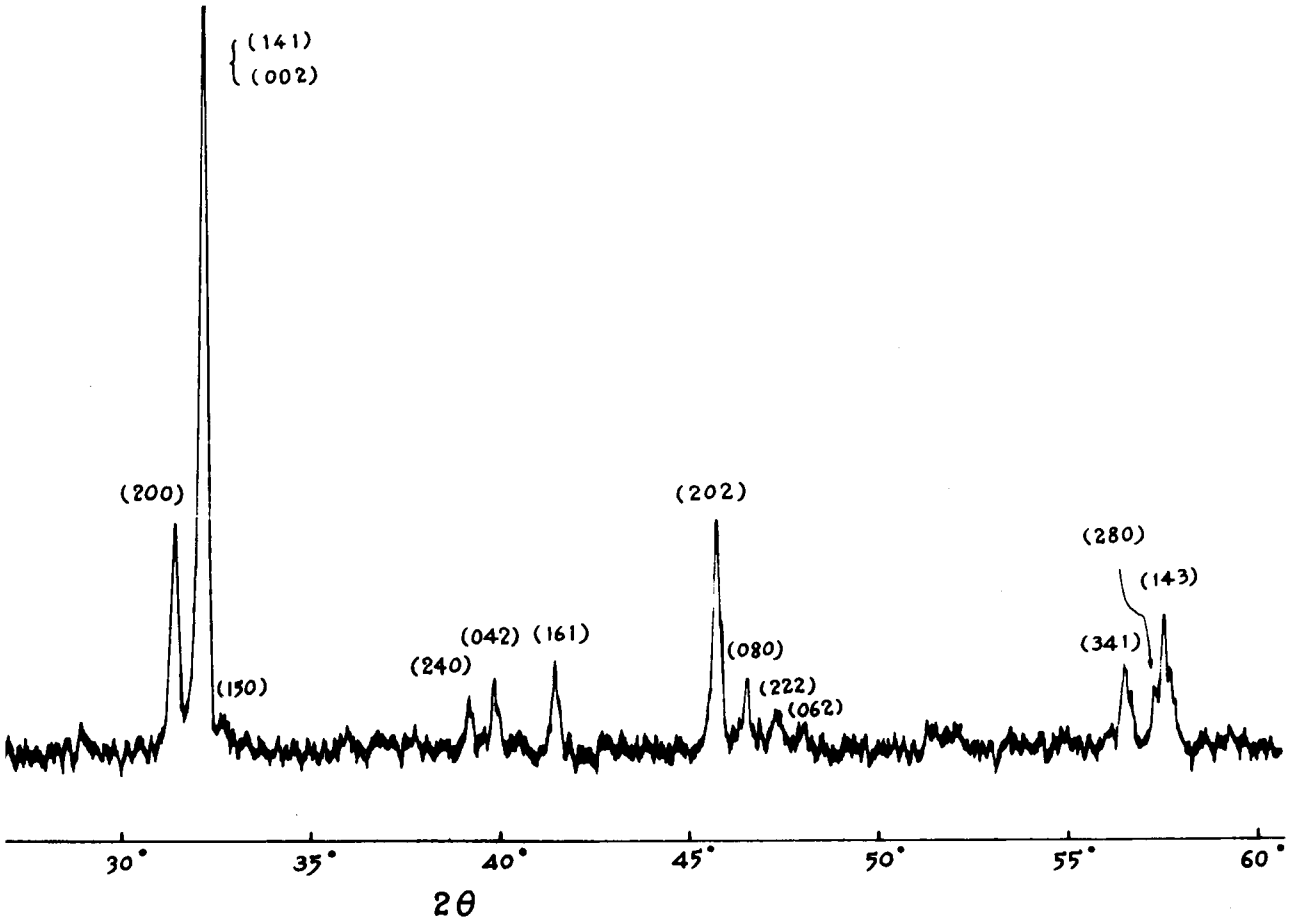

Fig. 4. X-ray (CuKα) diffractogram of the pyrolytic product of $SrFeO_{2.81}$.

In the measurement of lattice parameters of cubic or pseudo-cubic (tetragonal distortion) perovskites prepared, the {200} reflections were used. Silicon metal powder was used as an internal or external standard material. Scanning speeds used were $\frac{1}{4}^{\circ}$/min or $\frac{1}{8}^{\circ}$/min and 1cm/min.

4) ^{57}Fe Mössbauer spectrometry

Iron-57 Mössbauer spectra were measured for the system $(Ca_xSr_{1-x})FeO_{3-\delta}$ at room temperature in order to check the valence state of the iron ions as well as to investigate the relationship between the Mössbauer parameters and the chemical composition. Nearly 100 mg of sample was used as an absorber and 5μC of ^{57}Co embedded in copper was used as a source. Analysis was carried out by using two Mössbauer spectrometers, i.e., a Hitachi AA-40 Mössbauer Analyser attached with a 200-channel analyser, and "TMC Set" consisting of Gammascope 102, Drive Unit 306 and Transducer 305 operated in time mode. Calibrations were based on the quadrupole splitting of sodium nitroprusside $Na_2Fe(CN)_5NO\cdot 2H_2O$ and a value of 1.712 mm/sec[19] was used in the measurements of the velocity range of ±3 mm/sec. When the spectra of the brownmillerite-like compositions were measured in the velocity range of ±10 mm/sec, calibrations were based on the magnetic Zeeman splittings of α-Fe_2O_3[20] and pure Fe metal.[21] All isomer shifts of both Fe^{4+} and Fe^{3+} ions in each sample were relative to 310 stainless steel.

5) Measurements on magnetism and electricity

Magnetic susceptibilities of the perovskites $(Ca_xSr_{1-x})FeO_{3-\delta}$ were measured at temperatures ranging from liquid nitrogen temper-

ature to room temperature, because of the instability of the specimen at higher temperatures. All of the perovskites were essentially paramagnetic around room temperature. The measurements were made by using a Shimazu tortion magnetic balance in external magnetic fluxes up to 8000 Gauss. Faraday's method were applied for the measurements, using ca. 200 mg of sample and crystalline granules of pure $CuSO_4 \cdot 5H_2O$ as a standard material.[22] Estimation of the magnetic susceptibility χ_g and the intensity of magnetization σ_g were made based on the following equations.

$$F = m\chi_g H\frac{\partial H}{\partial x} = m\sigma_g\frac{\partial H}{\partial x}$$

where F is the specimen's force applied for magnetic balance, m the mass of sample, χ_g the magnetic susceptibility of 1 g of sample σ_g the intensity of magnetization of 1 g of sample, H an external magnetic field, and $\partial H/\partial x$ the external magnetic gradient in the direction of x-axis perpendicular to H.

Two-probe method was devised for the semi-quantitative measurement of electrical conductivities of the compositions $(Ca_xSr_{1-x})FeO_{3-\delta}$ at temperatures from liquid nitrogen temperature to room temperature. For the measurement ca. 200 mg of sample was pressed under a pressure of 150 Kg/cm^2. The pressed disk was ca. 2mm thick and 6mm in diameter. The electrodes of each specimen were coated with a silver-paint.

EXPERIMENTAL RESULTS

1) Chemical compositions

Table I summarizes the chemical compositions and the equilibrium conditions for the system $(Ca_xSr_{1-x})FeO_{3-\delta}$. These data imply that strontium-rich members of the system are effectively oxidized through the proposed high oxygen pressure process whereas dicalcium ferrite, $Ca_2Fe_2O_5$ (= $CaFeO_{2.5}$), is never oxidized to the perovskite composition. Another observation of the chemical composition of the system is worth mentioning. This concerns the temperature effect on the oxidation. As seen in Table I, the samples with x = 0, x = 0.2 and x = 0.4 equilibrated at an oxygen pressure of 120 atm and 300°C contain much more oxygens than those at almost the same oxygen pressure and 500°C. Such a tendency has been also observed in the system $SrFeO_{2.5-3.0}$ by MacChesney et al.[3] as seen in Fig. 5. The temperature effect may be explained in terms of high vaporizing pressure of oxygen at higher temperatures.

One other interesting correlation of oxygen deficiency with the fugacity of oxygen was found in a series of perovskites $(Ca_xSr_{1-x})FeO_{3-\delta}(0 \leqq x \leqq 0.4)$. When the reactant-resultant system is brought to equilibrium, then we have

$$\frac{1}{2}O_2\ (g) = O\ (s)$$

$$K = \frac{a_o\ (s)}{\sqrt{f_{O_2}}} \text{ or } a_o\ (s) = K\sqrt{f_{O_2}}\ ,$$

where K denotes the equilibrium constant for the system O_2 (g)-O (s), O_2 (g) gaseous oxygen molecule, O (s) the oxygen fraction in a solid-state anion-vacant perovskite $AFeO_{3-\delta}$, K the equilibrium

TABLE I. CHEMICAL COMPOSITIONS OF THE SYSTEM $(Ca_xSr_{1-x})FeO_{3-\delta}$.

Chemical compositions			Equilibration conditions		
x	3-δ	Fe^{4+}/Fe_{total} a) (%)	Oxygen pressure (atm)	Temperature (°C)	Time (hrs)
0 b)	2.77	54 c)	0.2	1100	6
0	2.81	62	0.2	1200	24 d)
0	2.85	70	30	500	24
0	2.91	82	120	500	24
0	2.94	88	780	500	24
0	2.97	94 c)	120	300	25
0	2.98	96	1850	500	25
0.2 b)	2.72	44 c)	0.2	1100	6
0.2	2.81	62	0.2	1200	24 d)
0.2	2.85	70	25	500	24
0.2	2.87	74	180	500	24
0.2	2.91	82	680	500	24
0.2	2.93	86 c)	120	300	24
0.2	2.99	98	1900	500	24
0.4	2.58	16	0.2	1200	24 d)
0.4	2.64	28 c)	0.2	1100	6
0.4	2.77	54	20	800	40
0.4	2.78	56	170	500	24
0.4	2.82	64	110	500	24

x	3-δ	(%)	(atm)	(°C)	(hrs)
0.4	2.86	72[c)]	120	300	24
0.4	2.87	74	610	500	24
0.4	2.90	80	1500	500	24
0.4	2.93	86	1850	500	24
0.6	2.54	8	0.2	1100	24
0.6	2.57	14[c)]	0.2	1100	6
0.6	2.59	18	40	500	24
0.6	2.67	34	150	500	24
0.6	2.77	54[c)]	120	300	24
0.6	2.83	66	1900	700	96
0.6	2.85	70	1500	450	24
0.8	2.51	2[c)]	0.2	1100	6
0.8	2.54	8[c)]	120	300	24
0.8	2.70	40	1500	500	67
1	2.50	0[c)]	0.2	1100	6
1	2.50	0[c)]	120	300	24
1	2.50	0	1400	500	40
1	2.50	0	1470	600	23

a) Most of the values were determined by thermogravimetric analysis. The experimental error was ±2% for Fe^{4+}.

b) These compositions were two-phase materials composed of perovskite phase as a main component and a trace of brownmillerite phase.

c) These compositions were determined by a redox volumetric analysis.

d) These starting materials were cooled with furnace after firing at 1200°C in the preparating process.

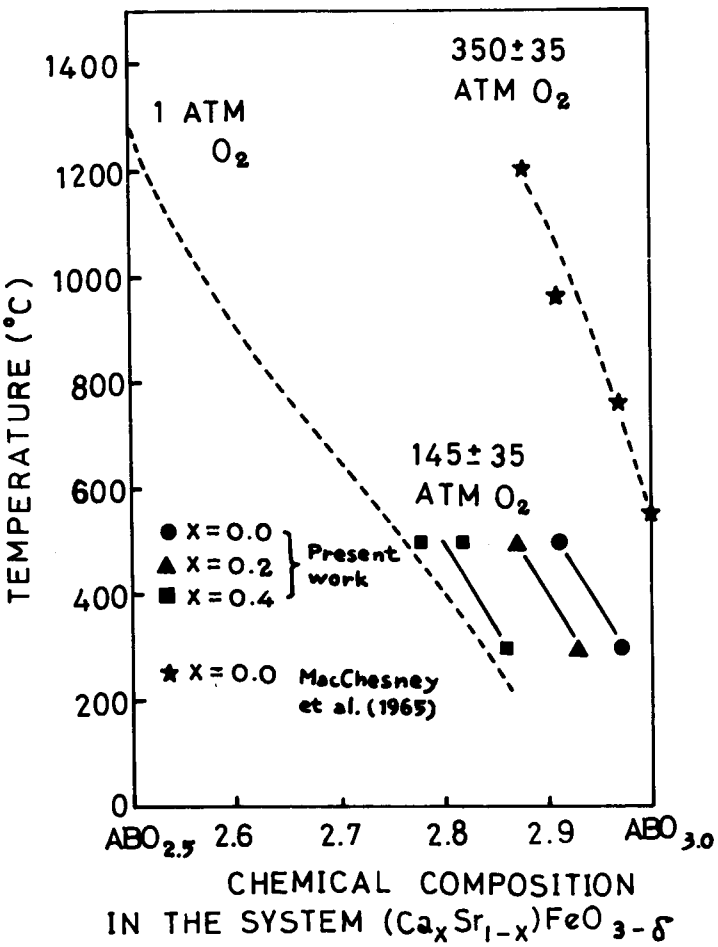

Fig. 5. Tentative phase diagram showing variation of compositions with temperature at 1 atm, 145 atm, and 350 atm oxygen pressures.

constant, a_o (s) the activity of oxygen in solid, and f_{O_2} the fugacity of oxygen. If the activity of oxygen (a_o (s)) is some function of the oxygen deficiencies in solid (δ), then it should be written by

$$a_o\ (s) = f\ (\delta) \propto \delta,$$

assuming a_o (s) has a linear correlation with δ. Thus, for the system O_2 (g)-O (s), it follows that

$$\delta \propto K' \sqrt{f_{O_2}}\ ,$$

where K' is a constant. From the plots of the square root of the fugacity of oxygen gas* vs. oxygen vacancy for a series of perovskites $(Ca_xSr_{1-x})FeO_{3-\delta}$ $(0 \leqq x \leqq 0.4)$ equilibrated with various oxygen pressures at 500°C for 24 hrs (see Fig. 6), the following experimental formula is derived:

$$\delta = K' \sqrt{f_{O_2}} + \delta_o\ ,$$

where δ_o defines the oxygen vacancies in a perovskite at the temperature of 500°C as the fugacity of oxygen gas approaches zero. Subsequently, the above formula could be expressed by the more precise one as follows:

---

* The fugacity of oxygen gas is obtained by the plots[23] of f/p vs. p_r, where f, p, and p_r represents the fugacity, pressure, and reduced pressure of a gas, respectively.

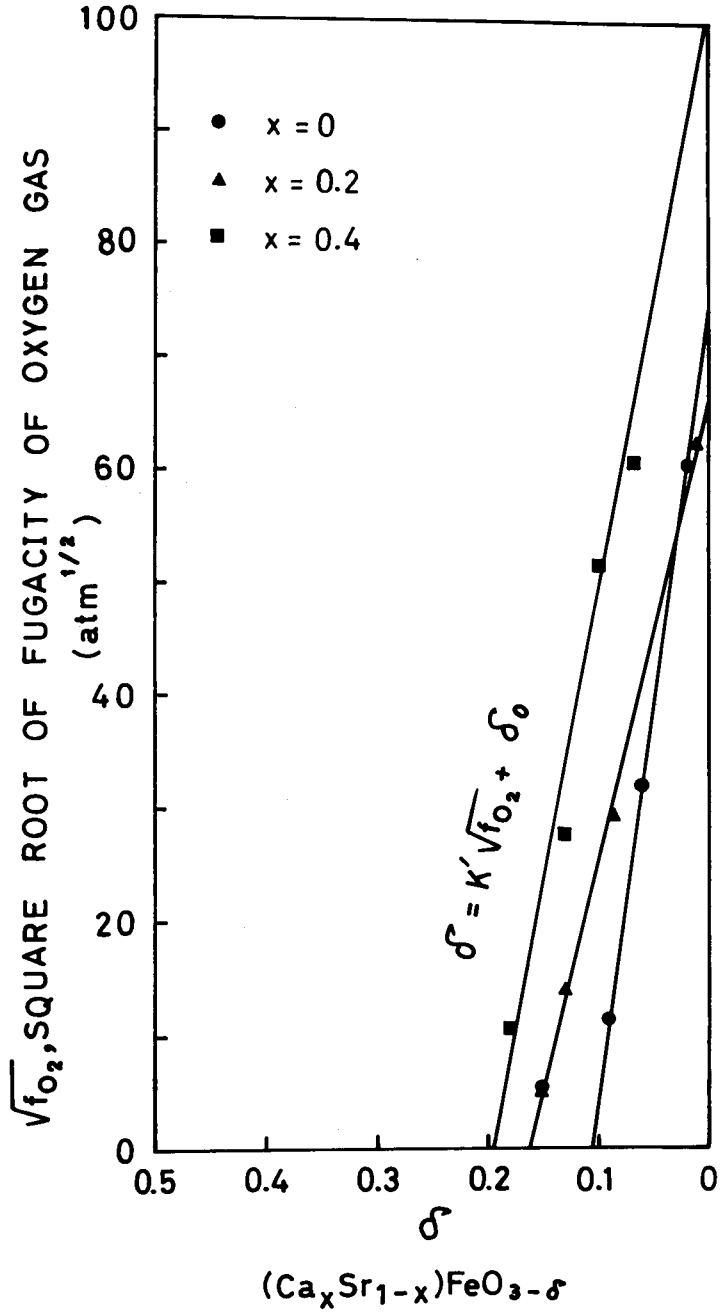

Fig. 6. Square root of the fugacity of oxygen gas vs. oxygen deficiency for a series of perovskites $(Ca_xSr_{1-x})FeO_{3-\delta}$ ($0 \leq x \leq 0.4$) equilibrated with various oxygen pressures at 500 °C for 24 hrs.

$$\delta\ (T) = K'\ (T)\ \sqrt{f_{O_2}} + \delta_o\ (T),$$

where T is the equilibrium temperature for the system. The average equilibrium constant K' (500°C) was determined for the present system and has a value of -4.25×10^{-3} $atm^{-1/2}$ $mole^{-1}$.

2) Phase identification and change of lattice parameters

Primary interest of the system $(Ca_xSr_{1-x})FeO_{3-\delta}$ is in the oxygen pressure effect on the resulting phases. Figure 7 shows the results obtained by X-ray diffractometry for the composition prepared at oxygen pressures of 0.2 atm (1100°C; 6 hrs) and 120 atm (300°C; 24 hrs). These products are characterized by the crystal structure; one is a modification of orthorhombic brownmillerite-like structure ($A_2Fe_2O_5$) and the other is that of cubic or pseudocubic perovskite-like structure ($AFeO_3$), if we stand A for Ca and/or Sr atoms. As shown in Fig. 7, the samples before oxidation have the $AFeO_3$ structure for x = 0 and x = 0.2 while those from x = 0.4 to x = 1 are of $A_2Fe_2O_5$ structure.

The starting materials, $(Ca_{0.8}Sr_{0.2})FeO_{2.51}$ and $CaFeO_{2.50}$, remained as the brownmillerite-like phases even by the intense oxidation at an oxygen pressure of 120 atm.

On the other hand, a striking conversion from $A_2Fe_2O_5$ to $AFeO_3$ structure appeared for the compositions, x = 0.4 and x = 0.6. Figure 8 shows the X-ray diffractograms of the materials $(Ca_{0.4}Sr_{0.6})FeO_{3-\delta}$ before and after oxidation. This structural change may be explained as that the incorporation of oxygen atoms in the lattice results in the increase of sixfold

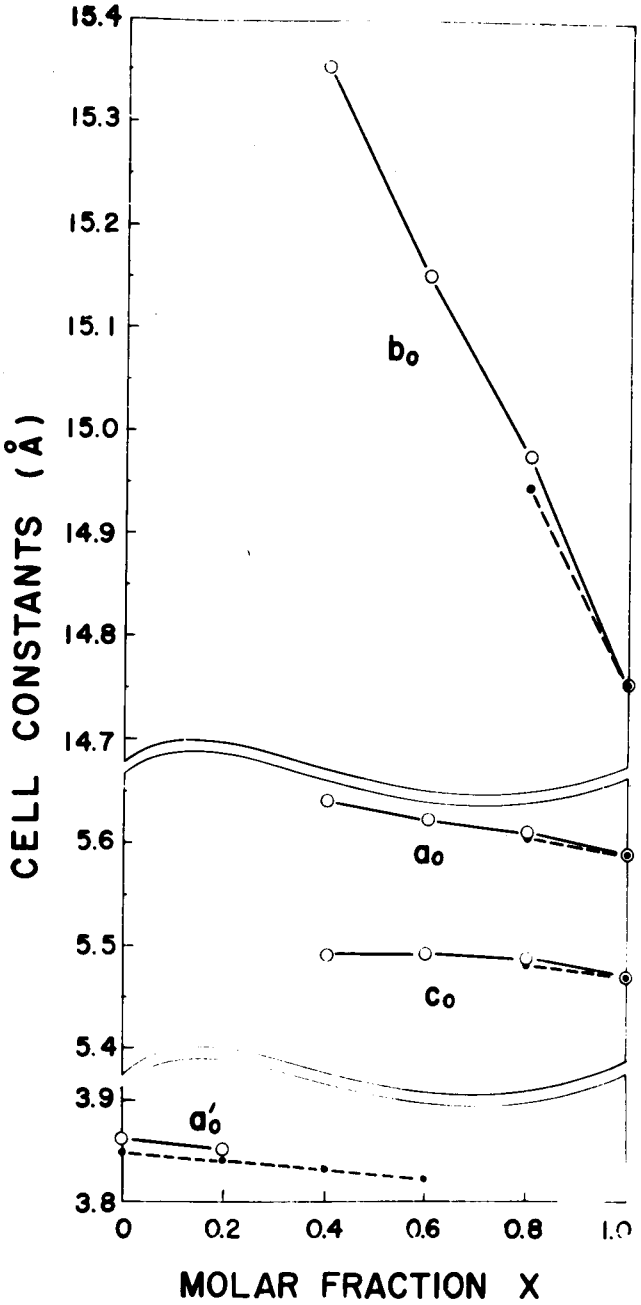

Fig. 7. Open and closed circles show cell constants for the system $(Ca_xSr_{1-x})FeO_{3-\delta}$ before and after oxidation, respectively, where a_o, b_o and c_o are those of an orthorhombic brownmillerite-like lattice, and a'_o is that of a cubic or pseudocubic perovskite lattice.

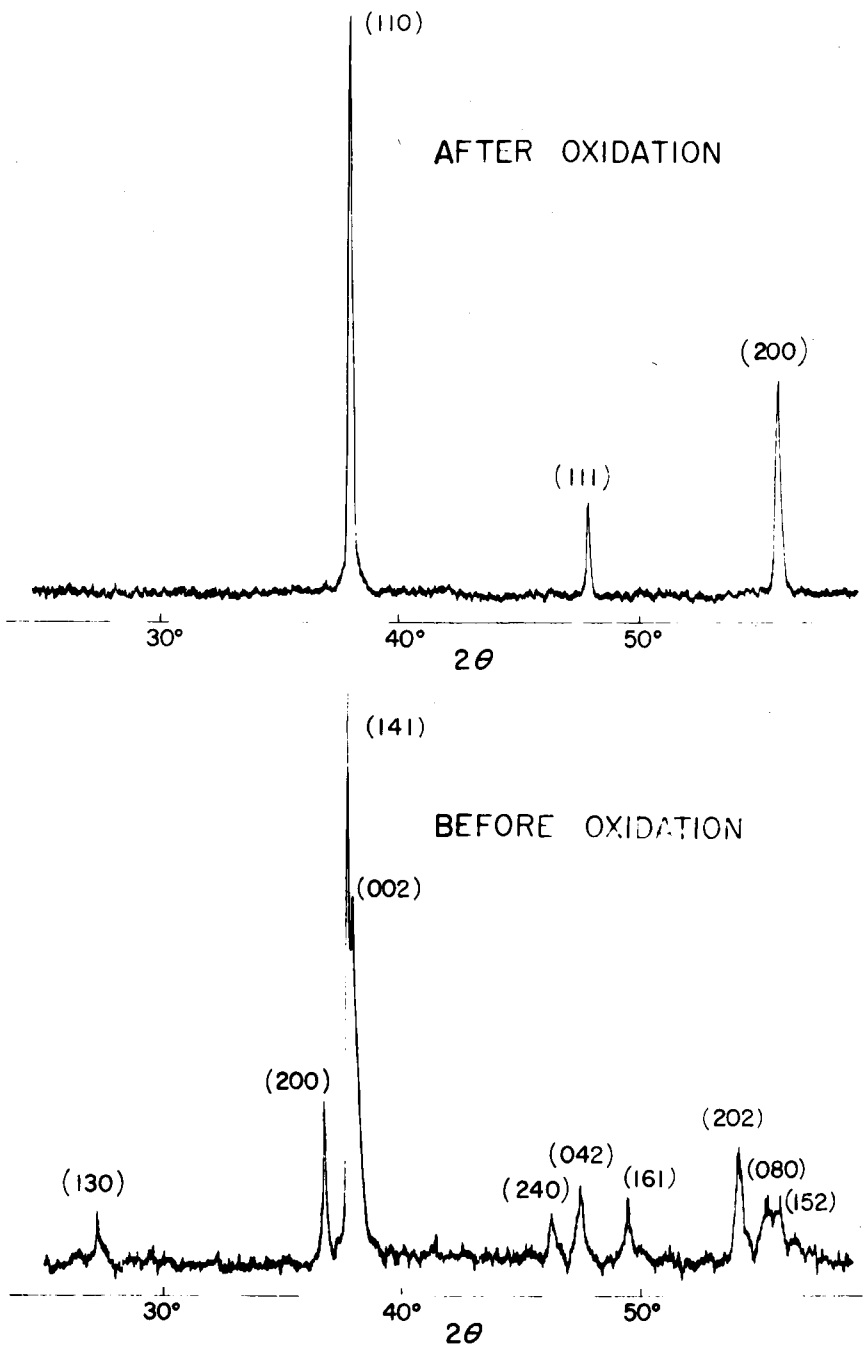

Fig. 8. X-ray (CoKα) diffractograms for specimens with the composition $(Ca_{0.4}Sr_{0.6})FeO_{3-\delta}$ before and after oxidation.

coordinated iron atoms in the lattice, followed by the pronounced change in crystal symmetry.

Of the compositions with x = 0 and x = 0.2, the samples before oxidation were pseudocubic (tetragonal) perovskite phases while the ones after oxidation were primitive cubic perovskites.

In order to investigate the tetragonal distortion of anion-deficient perovskites in detail, lattice parameters were measured for the perovskite compositions with x between 0 and 0.4 which were prepared at various oxygen pressures from 0.2 to 1900 atm and 500°C for 24 hrs. The results are depicted in Fig. 9. The data suggest that a-spacing shrinks with increasing Fe^{4+} concentration and characteristic tetragonal distortion occurs at the composition with Fe^{4+} between 60% and 64%. The similar results have been observed in the system $SrFeO_{2.5-3.0}$ by MacChesney et al.,[3] which are also pictured in Fig. 9. They have found that the compositions with 76-100% Fe^{4+} are simple cubic perovskites, the lattice parameters of which correlate linearly with their oxygen contents, while the more oxygen-deficient perovskites, i.e., $SrFeO_{2.72-2.84}$ (47-68% Fe^{4+}), demonstrates sizable tetragonal distortion.

Returning to the compositions with x = 0.8 and x = 1, it seems worthwhile to mention the results obtained when they were equilibrated at much higher oxygen pressures up to 1500 atm. The conversion from $A_2Fe_2O_5$ to $AFeO_3$ structure, as seen for the materials with x = 0.4 and x = 0.6, was not the case for dicalcium ferrite. However, the sample with x = 0.8 changed its chemical composition from $(Ca_{0.8}Sr_{0.2})FeO_{2.51}$ to $(Ca_{0.8}Sr_{0.2})FeO_{2.70}$ on

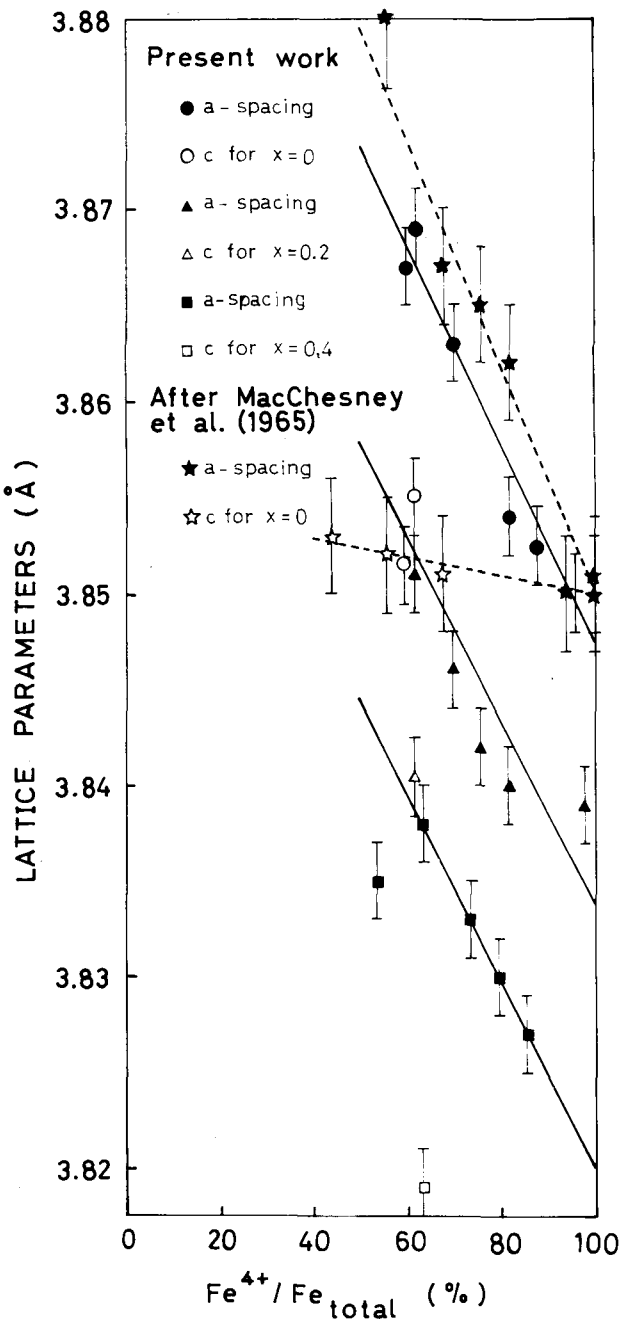

Fig. 9. Lattice parameters vs. the ratio Fe^{4+}/Fe_{total} for the system $(Ca_xSr_{1-x})FeO_{3-\delta}$ having the perovskite structure.

heating at an oxygen pressure of 1500 atm and 500°C for 67 hrs. Figure 10 shows the diffractogram of $(Ca_{0.8}Sr_{0.2})FeO_{2.70}$, which implies the formation of a perovskite phase though a trace of the starting material remained in the products.

3) Analysis of ^{57}Fe Mössbauer spectra

The purpose of this work is to examine the Mössbauer spectrum of iron in the oxygen deficient series $(Ca_xSr_{1-x})FeO_{3-\delta}$ $(0 \lesssim \delta \leqq 0.5)$. The spectrum of this series reflects differences in coordination of the iron ion, its valence state, and in its magnetic alignment. The present work demonstrates the efficacy of this experimental tool for detecting interactions between a specific ion and its coordination sphere.

The spectra of the perovskite phases are displayed in Figs. 11-15 and the partinent data are summarized in Table II.

Figure 11 presents the spectra for strontium ferrates with various anion-deficient perovskite compounds. The samples with nearly stoichiometric compositions-$SrFeO_{2.98}$ and $SrFeO_{2.94}$ show spectra composed of a sharp absorption line only. The observed isomer shifts are both +0.17 mm/sec relative to that of 310 stainless steel. Although the value is slightly larger than +0.15 mm/sec for $SrFeO_{3.0}$ which was measured by Gallagher et al.,[10] and +0.14 mm/sec for $SrFeO_{2.99}$ obtained by Shimony et al.,[11] the present value is fairly consistent with theirs within the error of ±0.03 mm/sec. A spectrum for $SrFeO_{2.85}$ is made up of two absorption lines corresponding to two different valence states of iron, i.e., Fe^{4+} and Fe^{3+}. The isomer shifts are +0.12 mm/sec

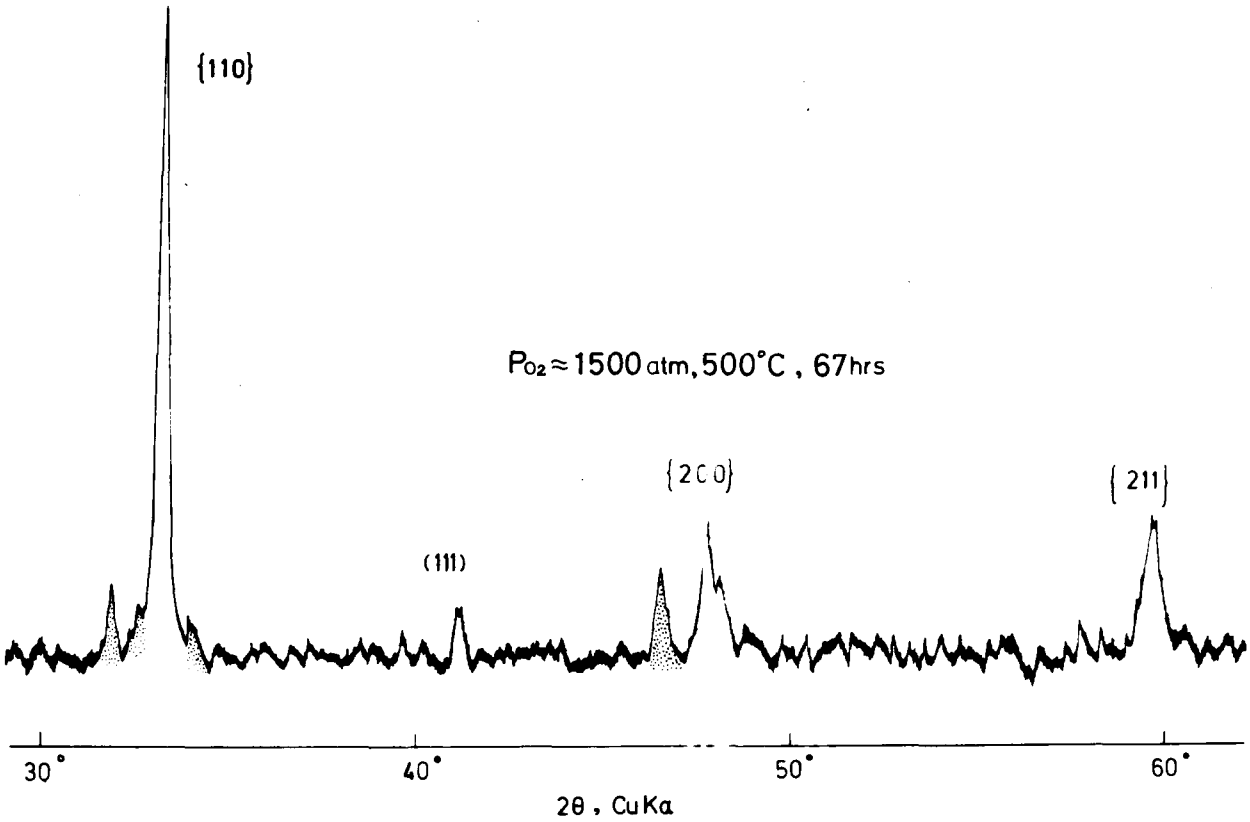

Fig. 10. X-ray diffractogram of $(Ca_{0.8}Sr_{0.2})FeO_{2.70}$. Dotted reflections are of a trace of the starting material.

TABLE II. Mössbauer parameters for perovskites in the system $(Ca_xSr_{1-x})FeO_{3-\delta}$.

Sample		Mössbauer parameters (mm/sec)*			
x	3-δ	Fe^{4+}		Fe^{3+}	
		IS	Quad.	IS	Quad.
0	2.81	-0.02	0.30	+0.79	0.53
0	2.85	+0.12	....	+0.46	....
0	2.91	+0.15	....	.....	....
0	2.94	+0.17	....	.....	....
0	2.98	+0.17	....	.....	....
0.2	2.81	+0.03	0.26	+0.83	0.53
0.2	2.85	+0.10	....	?**	....
0.2	2.87	+0.17	....	?**	....
0.2	2.91	+0.13	....	.....	....
0.2	2.99	+0.13	....	.....	....
0.4	2.77	0.00	0.30	+0.78	0.43
0.4	2.82	+0.03	0.23	+0.56	....
0.4	2.87	+0.10	....	+0.53	....
0.4	2.93	+0.13	....	+0.53	....
0.6	2.85	+0.10	....	+0.50	....

* The experimental error is ±0.03 mm/sec.

** These ferrates exhibited spectra of a broad asymmetric line profile. Therefore, the assignment of a Fe^{3+} absorption line was impossible for these compounds.

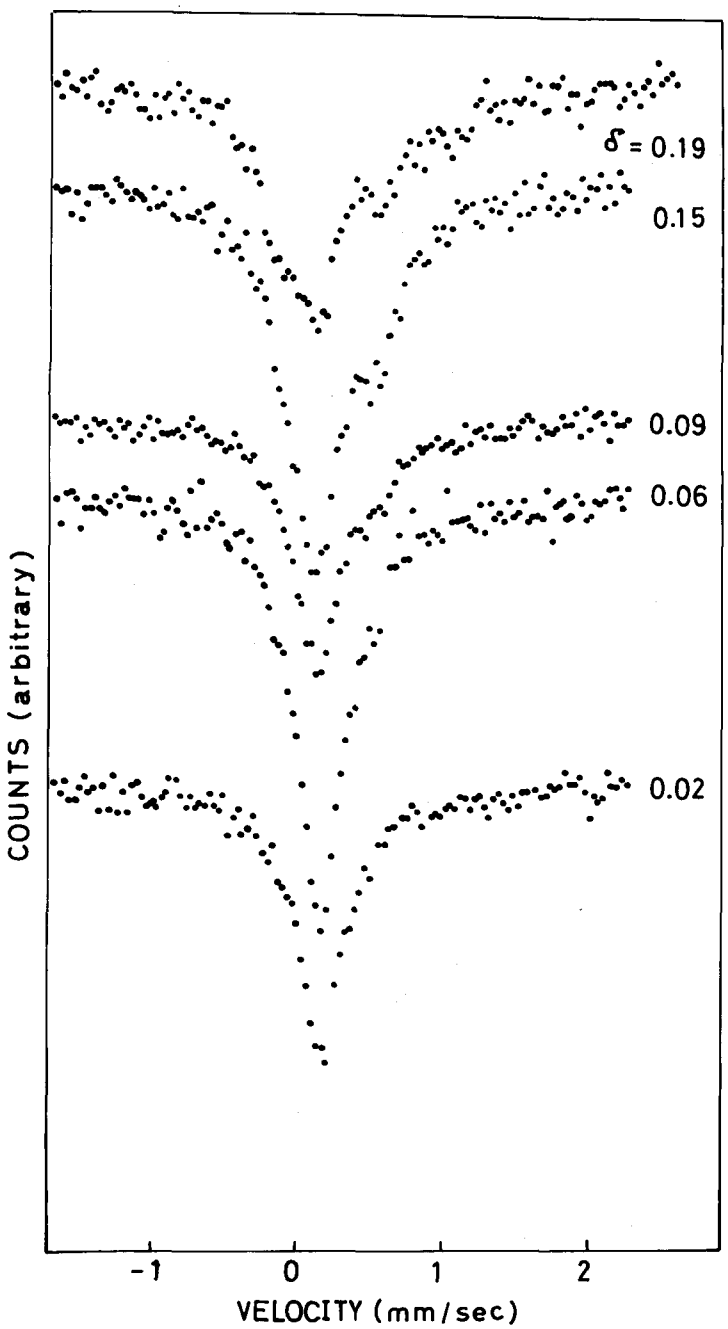

Fig. 11. Mössbauer spectra of $SrFeO_{3-\delta}$.

for Fe^{4+} and +0.50 mm/sec for Fe^{3+}. This is the material which is comparable to $SrFeO_{2.84}$ proposed by Shirane et al.[24] ($IS_{Fe^{4+}}$ = +0.10 mm/sec and $IS_{Fe^{3+}}$ = +0.55 mm/sec), Gallagher et al.[10] ($IS_{Fe^{4+}}$ = +0.12 mm/sec and $IS_{Fe^{3+}}$ = +0.58 mm/sec), and Shimony et al.[11] ($IS_{Fe^{4+}}$ = +0.10 mm/sec and $IS_{Fe^{3+}}$ = +0.71 mm/sec). These values previously obtained are not far from the values for the specimen $SrFeO_{2.85}$ in the present work.

The sample $SrFeO_{2.81}$ is of interest because it is still a single phase perovskite, but is significantly deficient in oxygen.

The anion deficiency leads to a tetragonal distortion of the lattice which was ascertained by X-ray diffractometry, i.e., c/a = 0.996. As expected, the spectrum shows quadrupole splittings for both Fe^{4+} and Fe^{3+} absorption lines. Their splitting energies are 0.30 mm/sec for Fe^{4+} and 0.53 mm/sec for Fe^{3+}.

The spectra of the samples $(Ca_{0.2}Sr_{0.8})FeO_{3-\delta}$ are shown in Fig. 12. The spectra are similar to those of strontium ferrates, but rather broad. Therefore, the assignment of Fe^{3+} absorption lines is difficult for the specimens with δ = 0.09, δ = 0.13 and δ = 0.15 in the series. The sample $(Ca_{0.2}Sr_{0.8})FeO_{2.81}$, accompanied by appreciable oxygen deficiencies, also shows measurable quadrupole splittings. The energies are 0.26 mm/sec for Fe^{4+} and 0.53 mm/sec for Fe^{3+}. The specimen $(Ca_{0.2}Sr_{0.8})FeO_{2.99}$, with the highest oxygen contents in the system, shows a single absorption line corresponding to that of Fe^{4+}. The isomer shift is +0.13 mm/sec.

The spectra of the series $(Ca_{0.4}Sr_{0.6})FeO_{3-\delta}$ are shown in

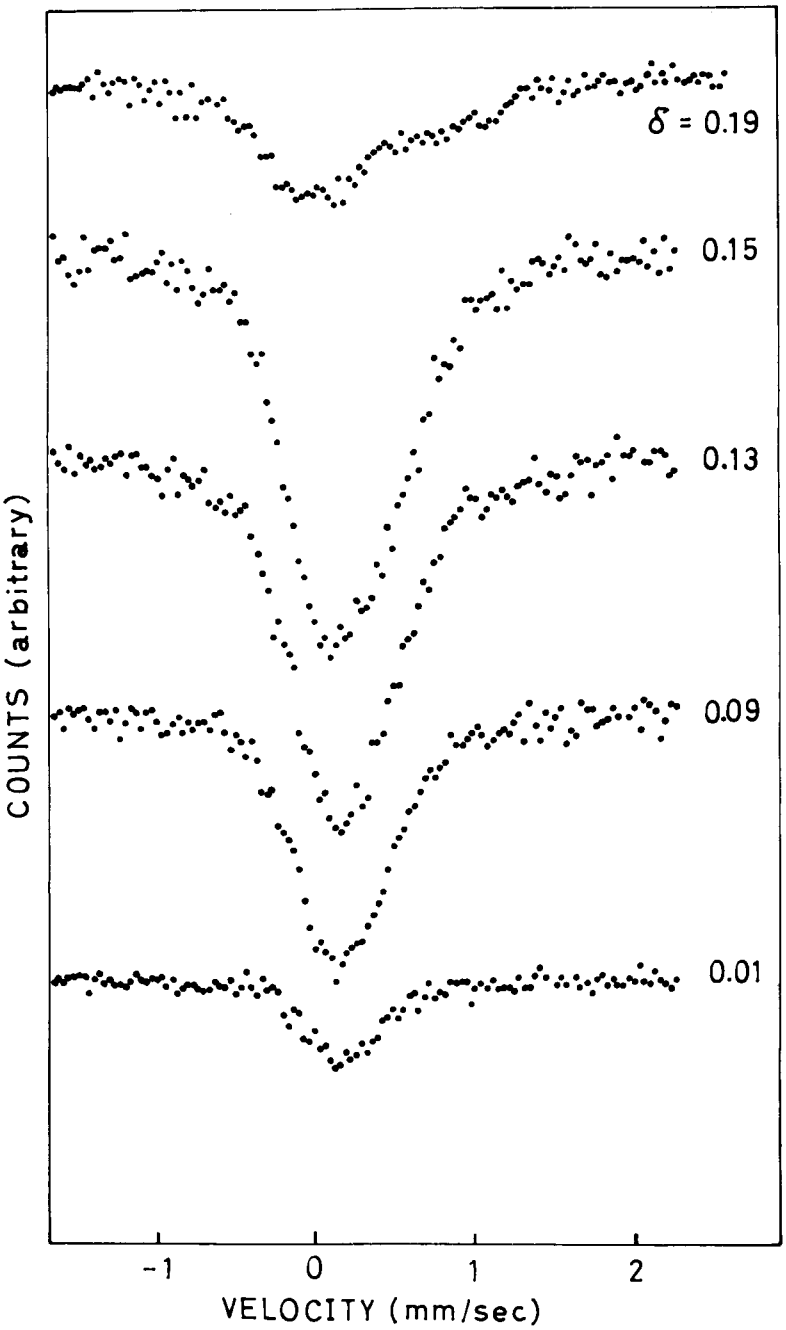

Fig. 12. Mössbauer spectra of $(Ca_{0.2}Sr_{0.8})FeO_{3-\delta}$.

Fig. 13. The spectra of the specimens with $\delta = 0.07$ and $\delta = 0.13$ are consisted of both Fe^{4+} and Fe^{3+} absorption lines, whose isomer shifts are +0.13 and +0.53 mm/sec for the former, and are +0.10 mm/sec and +0.53 mm/sec for the latter sample. The sample $(Ca_{0.4}Sr_{0.6})FeO_{2.77}$, with the lowest oxygen contents in the series, shows sizable quadrupole splittings for both Fe^{4+} and Fe^{3+}. The quadrupole splitting energies are 0.30 mm/sec and 0.43 mm/sec, respectively. On the other hand, the sample $(Ca_{0.4}Sr_{0.6})FeO_{2.82}$, with the second lowest oxygen contents, does not show a measurable quadrupole splitting for Fe^{3+}.

The spectra of the series $(Ca_{0.6}Sr_{0.4})FeO_{3-\delta}$ are shown in Fig. 14. The specimen $(Ca_{0.6}Sr_{0.4})FeO_{2.85}$, a single perovskite phase, shows a spectrum composed of Fe^{4+} and Fe^{3+} absorption lines. The isomer shifts are +0.10 mm/sec for Fe^{4+} and +0.50 mm/sec for Fe^{3+}. The spectrum of the starting material $(Ca_{0.6}Sr_{0.4})FeO_{2.54}$ is depicted in Fig. 15. The X-ray powder pattern of this material was indexed by reference to its presumed isomorph, $CaFeO_{2.5}$ brownmillerite, though the chemical composition implies the coexistence of a trace of perovskite phase in the material. Figure 16[16] shows a projection of this structure consisting of alternate layers of iron(III) in octahedral and tetrahedral configurations, which is consistent with the observed Mössbauer effect. However, the discrete absorption lines (dashed lines in Fig. 15) are recognized in the spectrum besides the double six absorption lines of iron(III). These additional lines seem to be those of perovskite phase, which co-exists in the sample as expected from the chemical

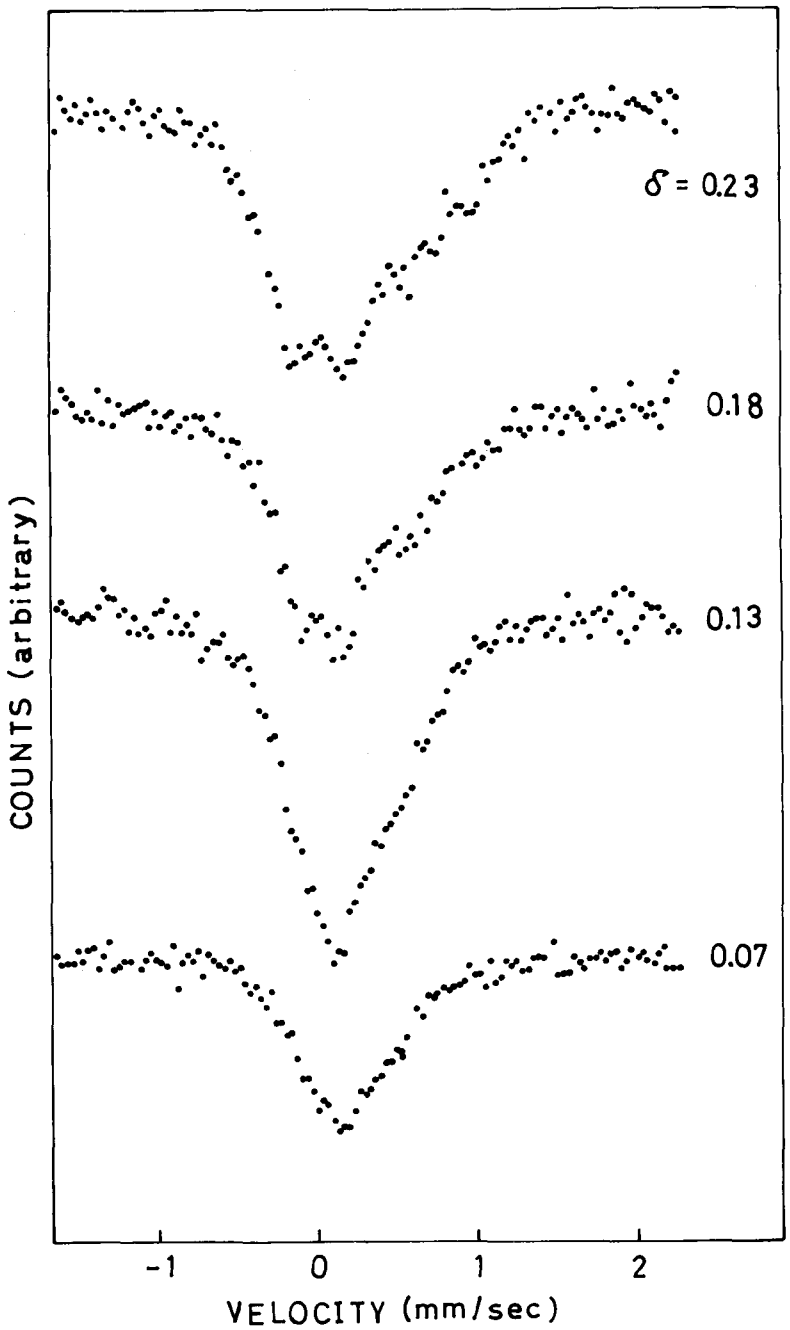

Fig. 13. Mössbauer spectra of $(Ca_{0.4}Sr_{0.6})FeO_{3-\delta}$.

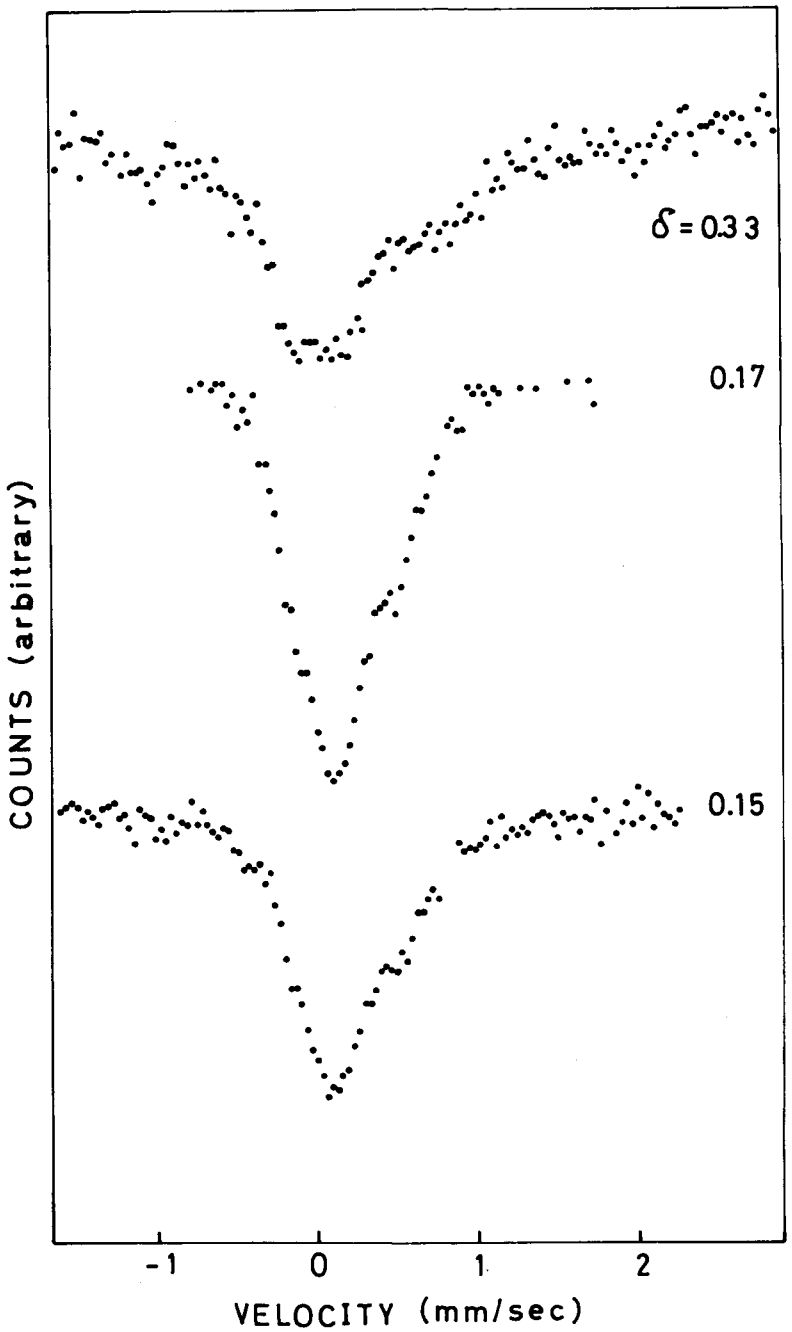

Fig. 14. Mössbauer spectra of $(Ca_{0.6}Sr_{0.4})FeO_{3-\delta}$.

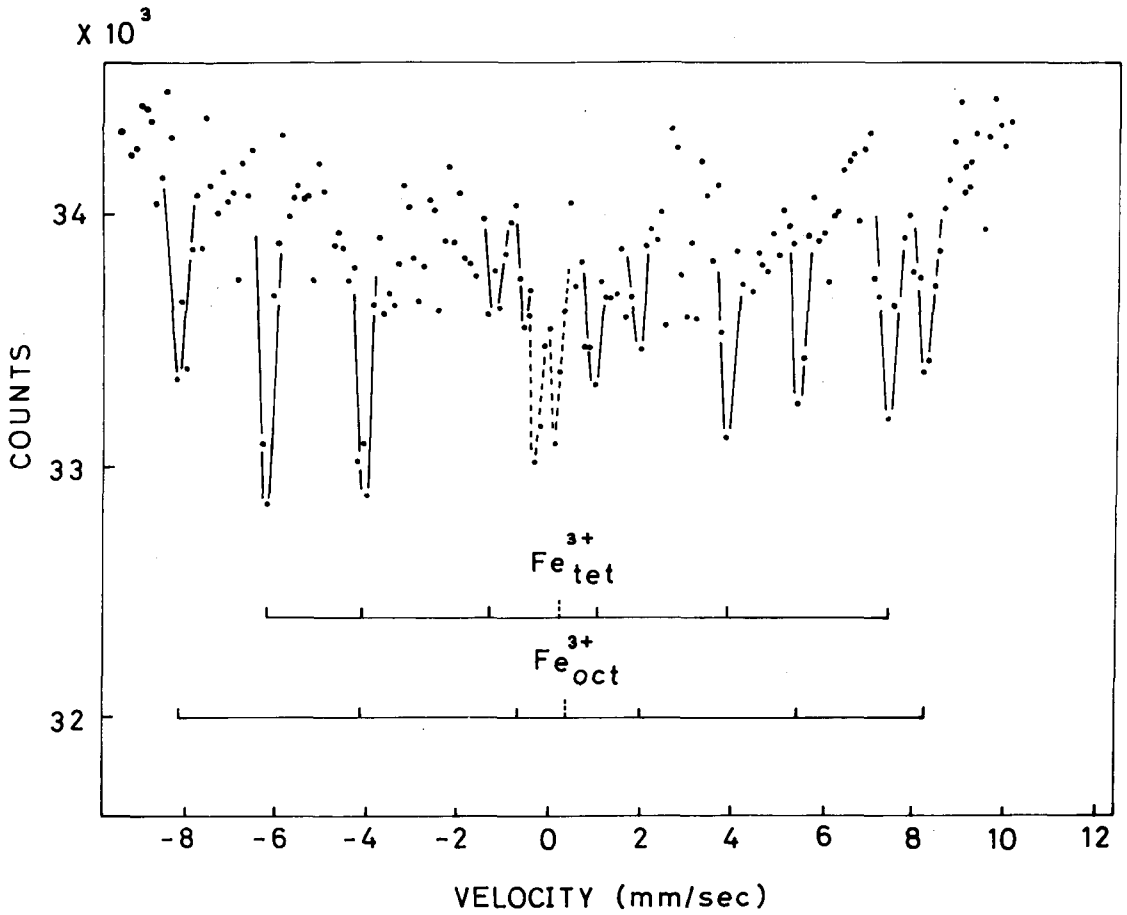

Fig. 15. Mössbauer spectrum of $(Ca_{0.6}Sr_{0.4})FeO_{2.54}$. Dashed line shows the absorption of the perovskite-phase impurity.

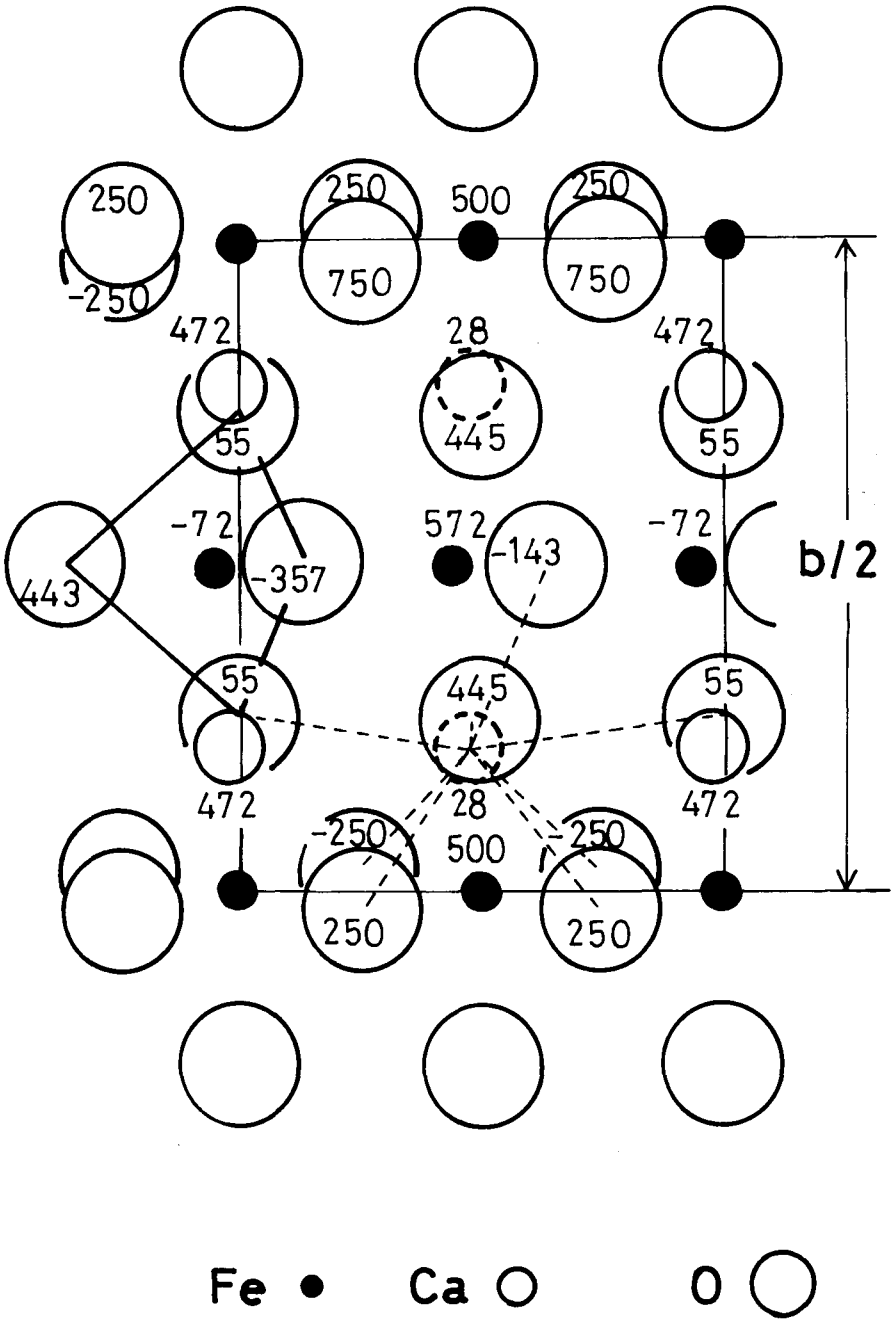

Fig. 16. Structure of brownmillerite-like dicalcium ferrite ($Ca_2Fe_2O_5$ or $CaFeO_{2.5}$) projected perpendicular to the c-axis.

composition.

The sample $(Ca_{0.8}Sr_{0.2})FeO_{2.70}$ is of interest because it is also a mixture of perovskite and brownmillerite phases. However, the spectrum shows only a paramagnetic Mössbauer response as seen in Fig. 17. The two resonance peaks are assigned to as those of perovskite phase, based on the similarity of the spectrum with that of strontium ferrate(IV). The isomer shifts of Fe^{4+} and Fe^{3+} are +0.17 mm/sec and +0.62 mm/sec, respectively.

Of one of the end members of the present system, i.e., calcium ferrate, the spectra before and after oxidation are pictured in Fig. 18. The data show that any measurable effect of high oxygen pressure on the ferrate is not recognized and only antiferromagnetic responses of the iron(III) at tetrahedral and octahedral sites appear in the spectra,[25)-28)] corresponding to the crystal structure.

4) Magnetic and electric properties

Interest here was initiated by Jonker and Van Santen's discovery of ferromagnetism exhibited by the orthomanganites and orthocobaltites.[29)] The former case appears to have been extensively investigated[30), 31)] and is explained in terms of superexchange[32)] and semi-covalent exchange[30)] between the Mn^{3+} ion and other 3d ions.

Because the Fe^{4+} ion is isoelectronic with Mn^{3+}, both having the $3d^4$ configuration, compounds containing this ion have been investigated. Of these, strontium ferrate has received the greatest attention even though it was not (previously) obtained as nominally stoichiometric $SrFeO_3$. Recently MacChesney et al.[3)]

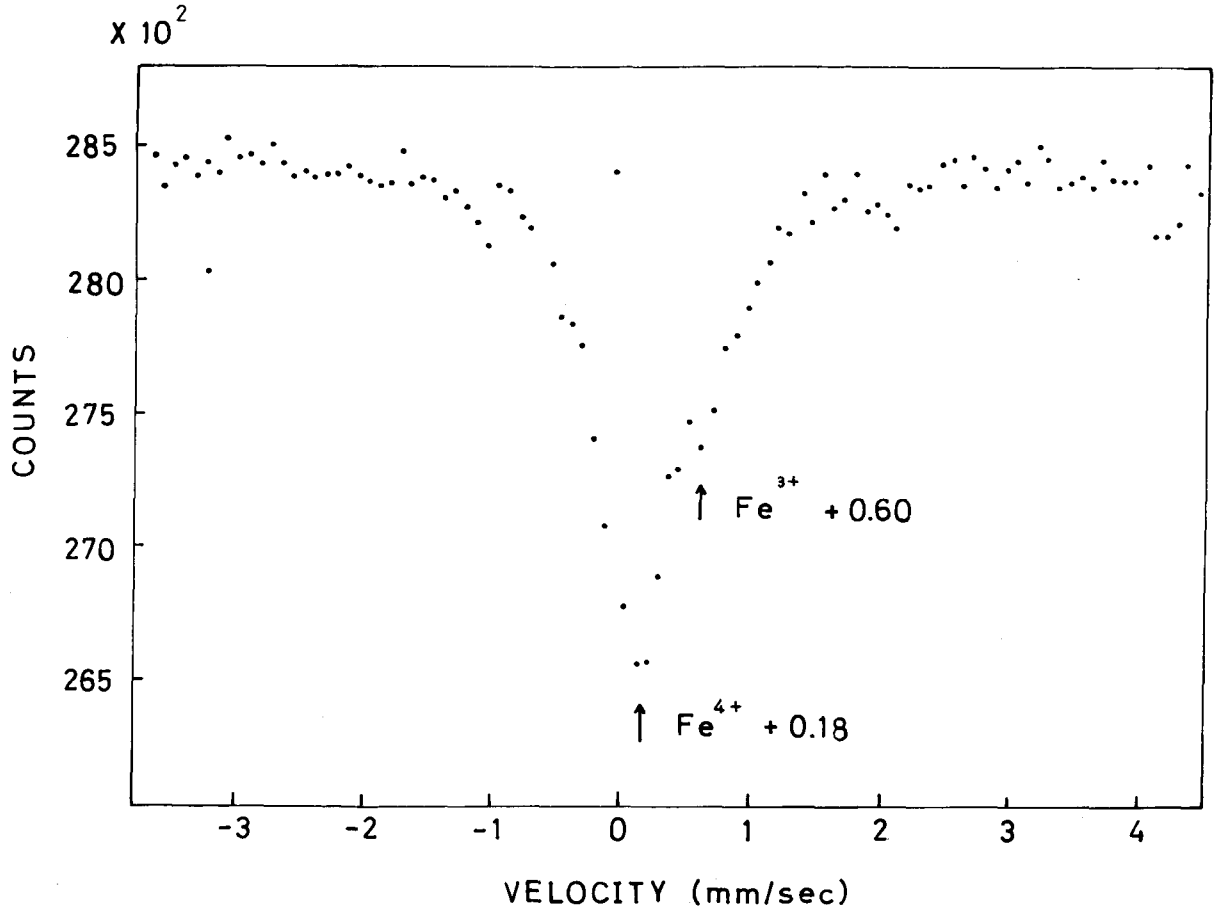

Fig. 17. Mössbauer spectrum of $(Ca_{0.8}Sr_{0.2})FeO_{2.70}$.

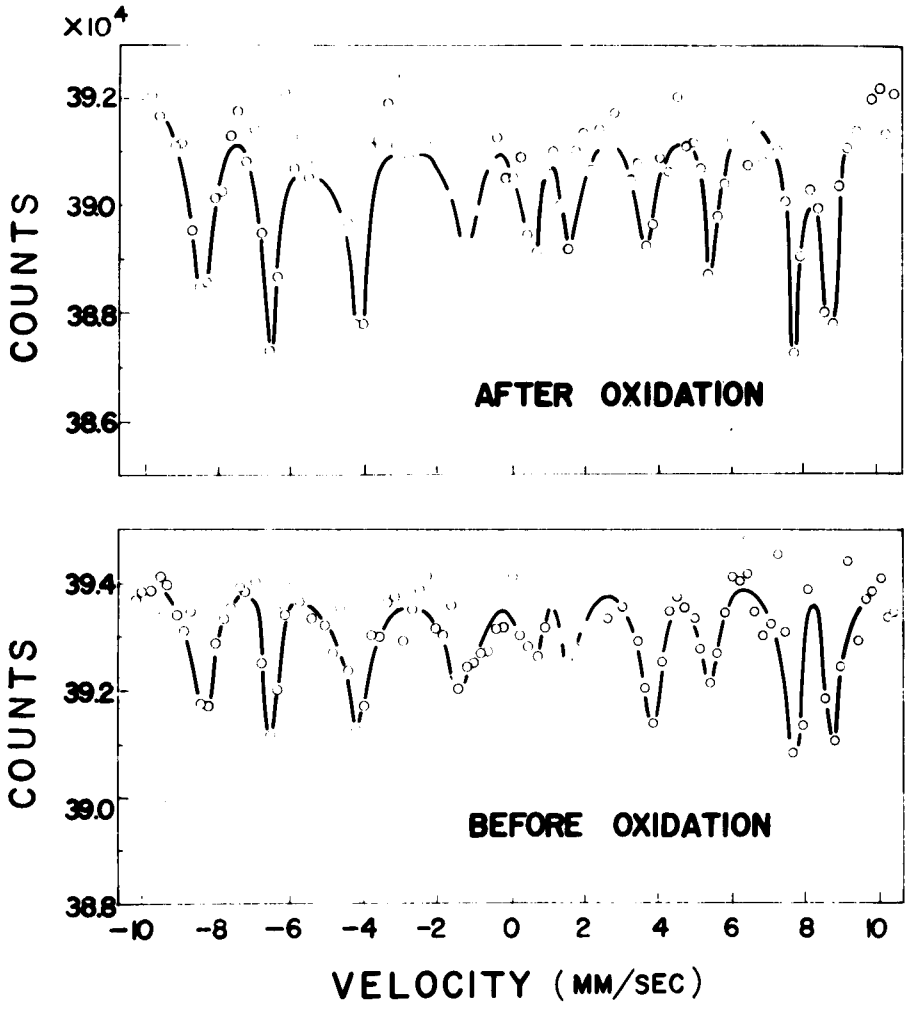

Fig. 18. Mössbauer spectra of calcium ferrates before and after oxidation.

have prepared strontium ferrates with various oxygen contents and measured their electric and magnetic properties. They have found that the material $SrFeO_{3.0}$ exhibit rather high conductivity ($\sigma = 5 \times 10^2$ mho·cm^{-1}), and also antiferromagnetic character with a Néel temperature of 130°K. It has also been found that the reciprocal susceptibility-temperature curve gives an anomalously high effective paramagnetic moment of 6.3 Bohr magnetons.

In the present paper, the author intended to examine the magnetic and electric properties of the system $(Ca_xSr_{1-x})FeO_{3-\delta}$ ($0 \leqq x \leqq 0.6$; $0 \lesssim \delta \lesssim 0.2$) with the perovskite structure at the temperatures ranging from liquid N_2 temperature to room temperature, in order to study the abnormal characteristics in magnetism and electricity also for the system.

Curves of reciprocal molar susceptibility ($1/\chi_m$) vs. temperature for $SrFeO_{2.81}$, $SrFeO_{2.85}$, $SrFeO_{2.91}$, $SrFeO_{2.94}$, and $SrFeO_{2.98}$ are shown in Fig. 19. The temperature at which the trough in these curves occurs decreases and the trough broadens as the Fe^{4+} concentration decreases to $SrFeO_{2.85}$. The most anion-deficient sample, $SrFeO_{2.81}$, does not demonstrate any Néel temperature above 77°K, whereas the near-stoichiometric perovskites, $SrFeO_{2.81-2.98}$, have an apparent Néel temperature of ca. 110°K. All of the compositions in the system $SrFeO_{2.81-2.98}$ measured, except for $SrFeO_{2.94}$, have a positive paramagnetic Curie temperature.

Figure 20 shows the plots of $1/\chi_m$ vs. temperature for $(Ca_{0.2}Sr_{0.8})FeO_{2.85-2.99}$. Either specimen has not ever any Néel temperature in the temperature range studied, but has a positive paramagnetic temperature.

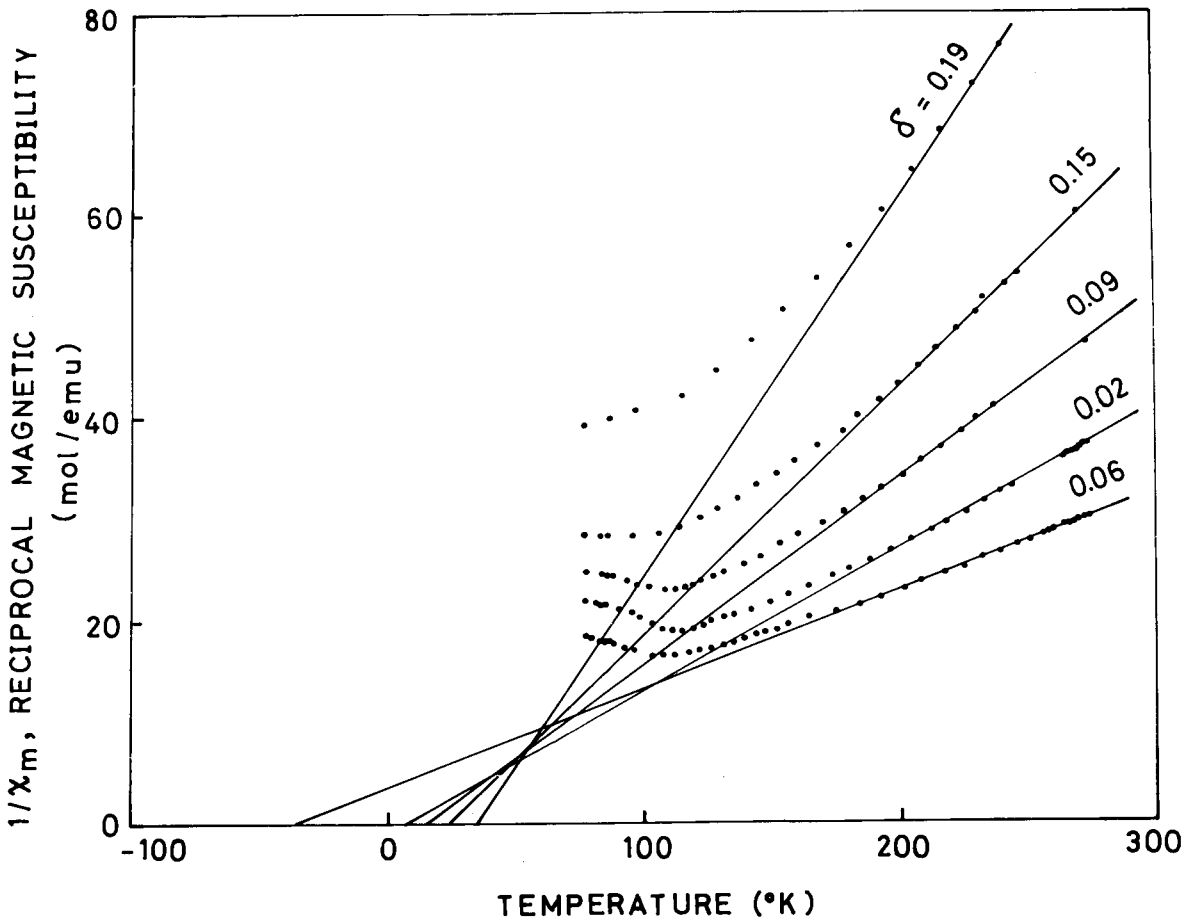

Fig. 19. Reciprocal magnetic susceptibility vs. temperature for $SrFeO_{3-\delta}$.

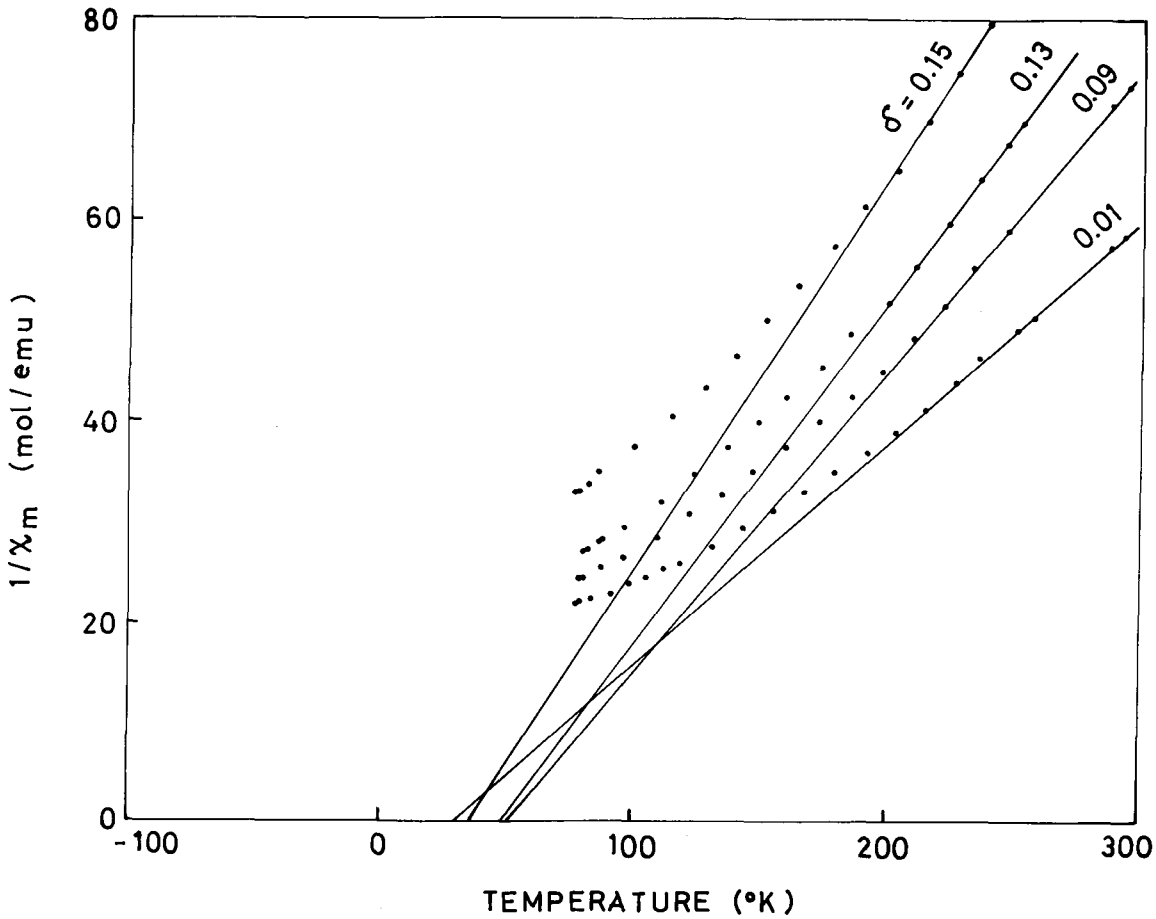

Fig. 20. Reciprocal magnetic susceptibility vs. temperature for $(Ca_{0.2}Sr_{0.8})FeO_{3-\delta}$.

Figure 21 illustrates the results for $(Ca_{0.4}Sr_{0.6})FeO_{2.77-2.93}$. The two ultimate compositions, $\delta = 0.07$ and $\delta = 0.23$, have negative paramagnetic Curie temperatures while the intermediates take positive values. The present measurements failed to find the Néel temperature of these materials.

Finally a plot of $1/\chi_m$ vs. temperature for the composition $(Ca_{0.6}Sr_{0.4})FeO_{2.83}$ is displayed in Fig. 22. The paramagnetic Curie temperature for the sample is negative. The experimental magnetic parameters for these perovskites are summerized in Table III.

Electrical resistivities were measured semi-quantitatively for several compositions in the system $(Ca_xSr_{1-x})FeO_{3-\delta}(0 \leqq x \leqq 0.6)$ by using a two-probe method. The resistivities are plotted as a function of 1000/T in Figs. 23-27, where T is absolute temperatue.

As shown in Figs. 23-27, the resistivities for the perovskite compositions in the system $(Ca_xSr_{1-x})FeO_{3-\delta}(0 \leqq x \leqq 0.6)$ tend to become temperature-independent, especially at the temperatures below ca. 100°K, while $(Ca_{0.4}Sr_{0.6})FeO_{2.58}$ with the brownmillerite-like structure clearly demonstrates a typical semiconductive behavior (see Fig. 27).

DISCUSSIONS

1) Crystal chemistry

The plots of the lattice parameters of perovskite compositions in the system $(Ca_xSr_{1-x})FeO_{3-\delta}(0 \leqq x \leqq 0.4;\ 0.01 \leqq \delta \leqq 0.19)$ as a function of Fe^{4+} concentration, which are displayed in Fig. 9,

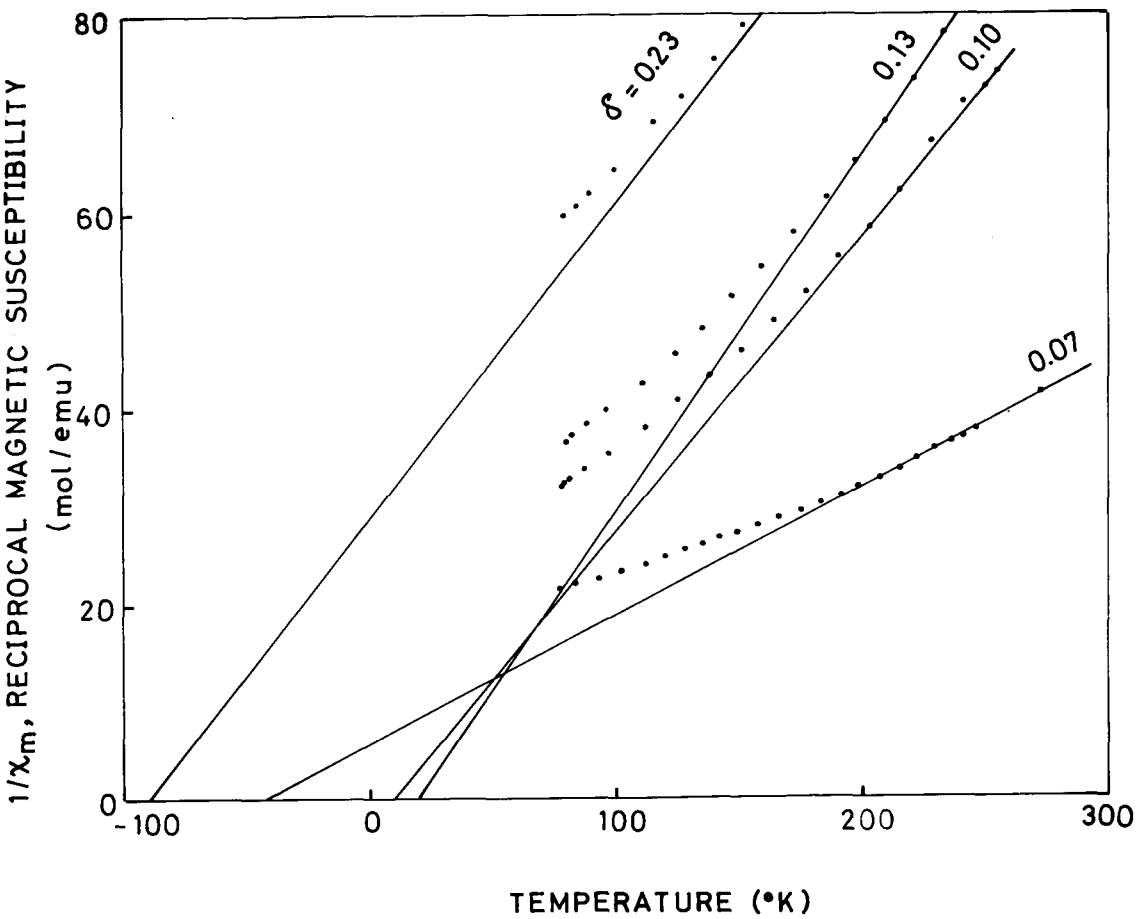

Fig. 21. Reciprocal magnetic susceptibility vs. temperature for $(Ca_{0.4}Sr_{0.6})FeO_{3-\delta}$.

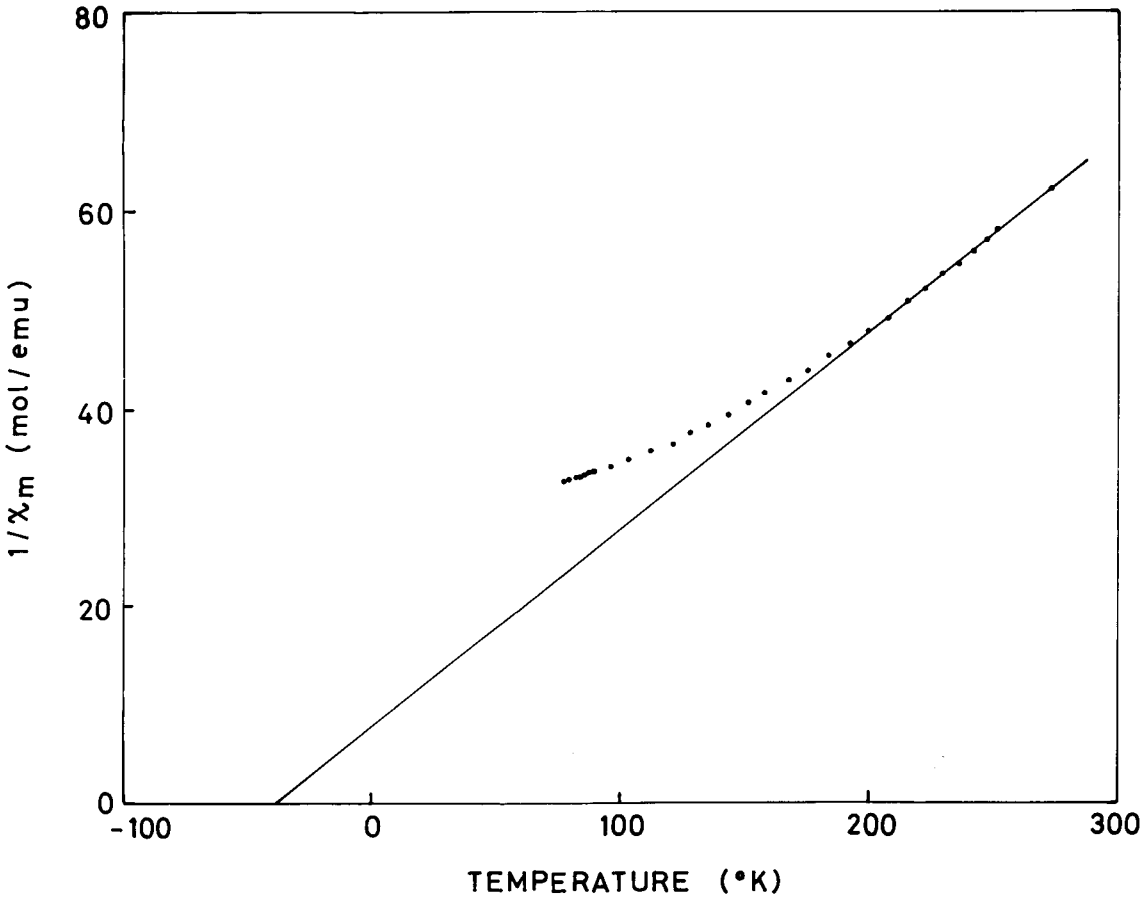

Fig. 22. Reciprocal magnetic susceptibility of $(Ca_{0.6}Sr_{0.4})FeO_{2.83}$ vs. temperature.

TABLE III. MAGNETIC PARAMETERS FOR PEROVSKITES

$(Ca_xSr_{1-x})FeO_{3-\delta}$ $(0 \leqq x \leqq 0.6;\ 0.01 \leqq \delta \leqq 0.19)$

Compositions		Magnetic parameters		
x	3-δ	T_N (°K)*	θ (°K)**	C_m***
0	2.81	< 77	36	2.67
0	2.85	ca.80	23	4.11
0	2.91	110	14	5.50
0	2.94	107	-40	10.43
0	2.98	115	6	7.17
0.2	2.85	< 77	36	2.58
0.2	2.87	< 77	48	2.93
0.2	2.91	< 77	50	3.34
0.2	2.99	< 77	30	4.50
0.4	2.77	< 77	-90	3.13
0.4	2.87	< 77	20	2.72
0.4	2.90	< 77	10	3.30
0.4	2.93	< 77	-44	7.61
0.6	2.83	< 77	-38	5.01

* Experimental errors are ±5°K.

** Experimental errors are ±10°K.

*** The maximum error for C_m, estimated from θ and χ_m, is ±0.35.

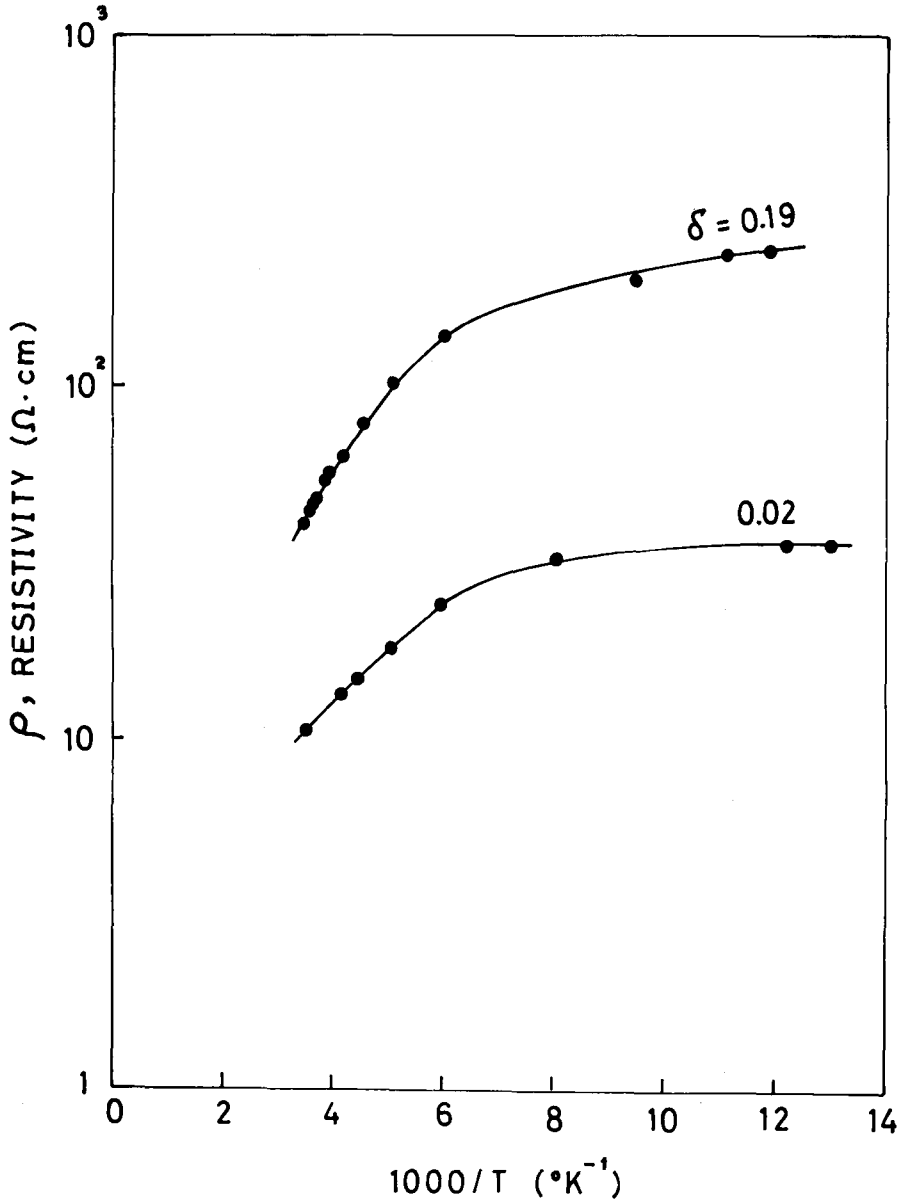

Fig. 23. Log. electrical resistivity vs. reciprocal temperature for $SrFeO_{3-\delta}$.

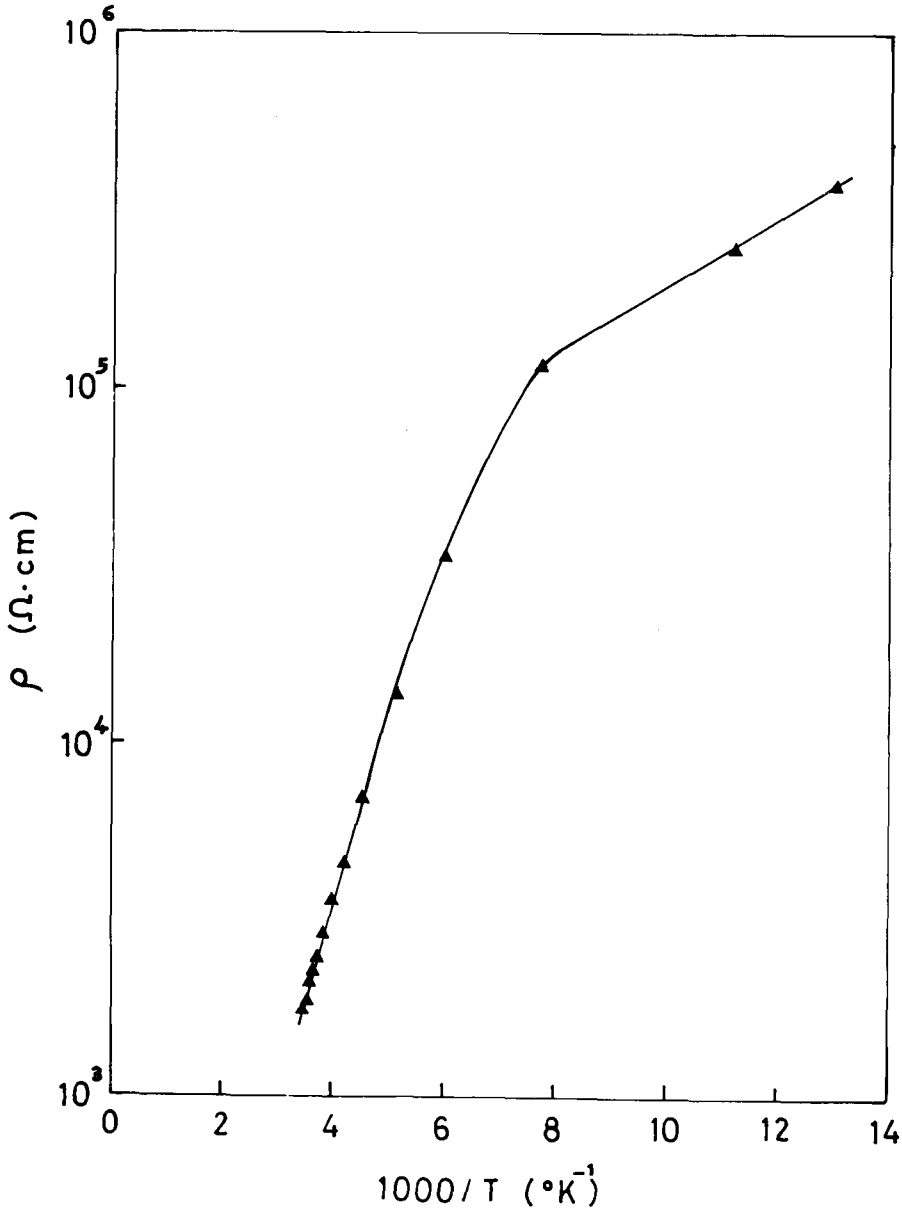

Fig. 24. Log. electrical resistivity of $(Ca_{0.2}Sr_{0.8})FeO_{2.85}$ vs. reciprocal temperature.

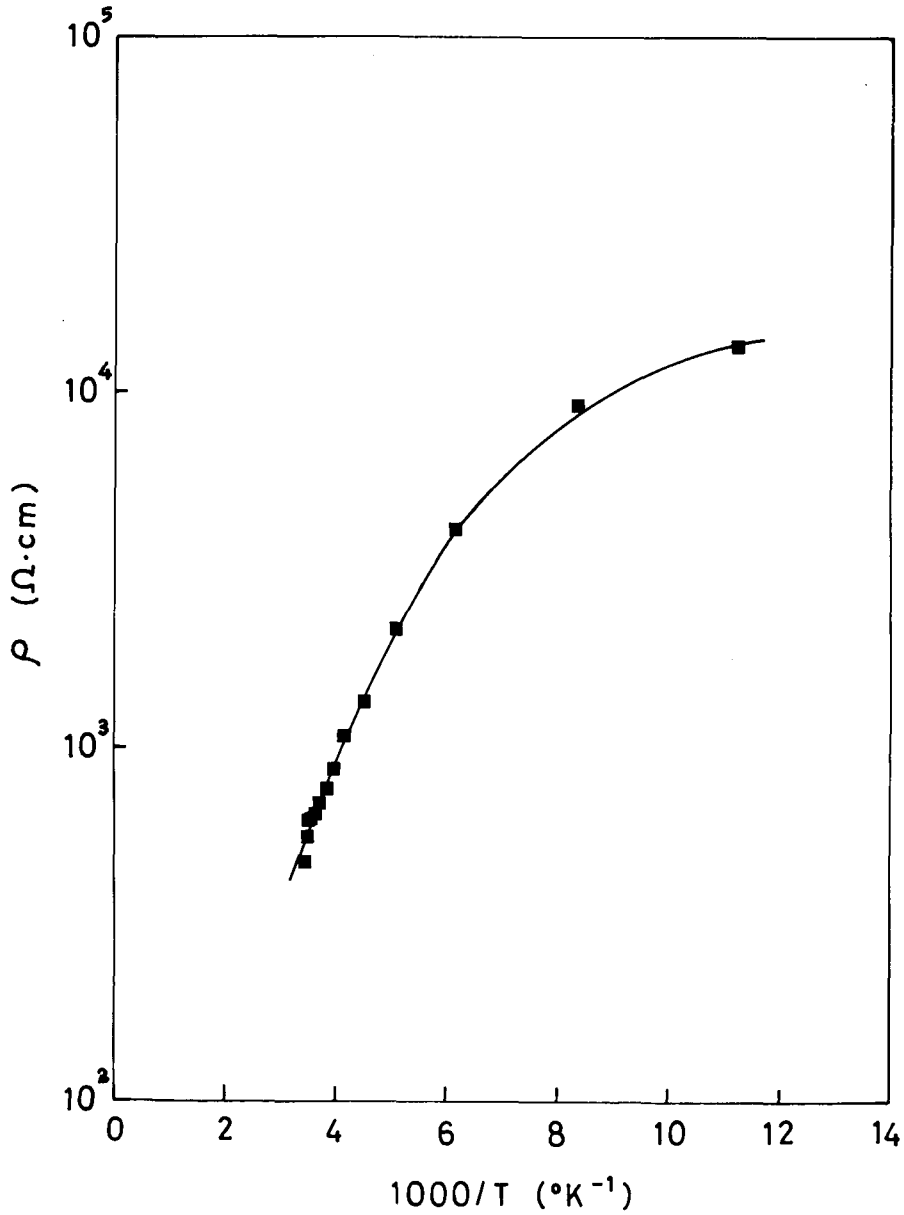

Fig. 25. Log. electrical resistivity of $(Ca_{0.4}Sr_{0.6})FeO_{2.93}$ vs. reciprocal temperature.

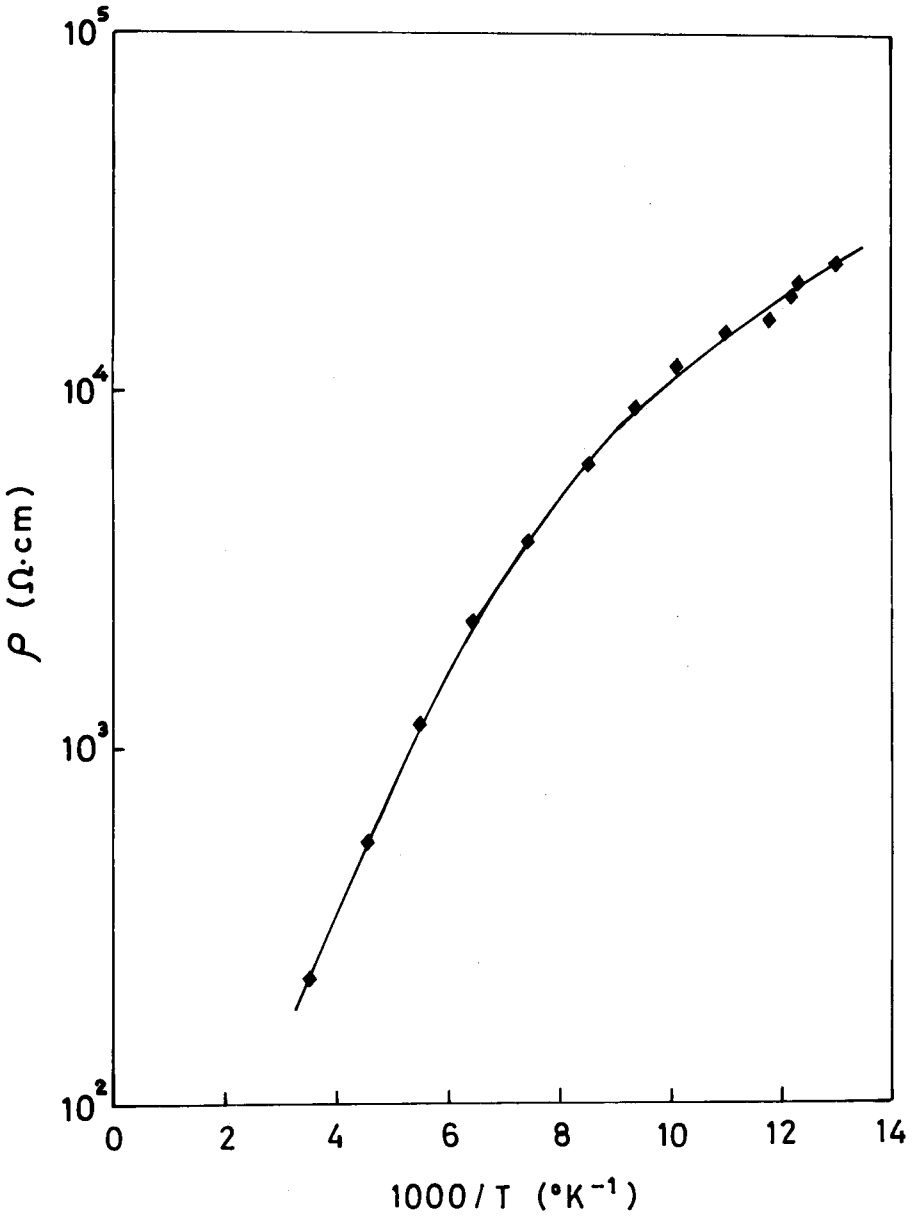

Fig. 26. Log. electrical resistivity of $(Ca_{0.6}Sr_{0.4})FeO_{2.83}$ vs. reciprocal temperature.

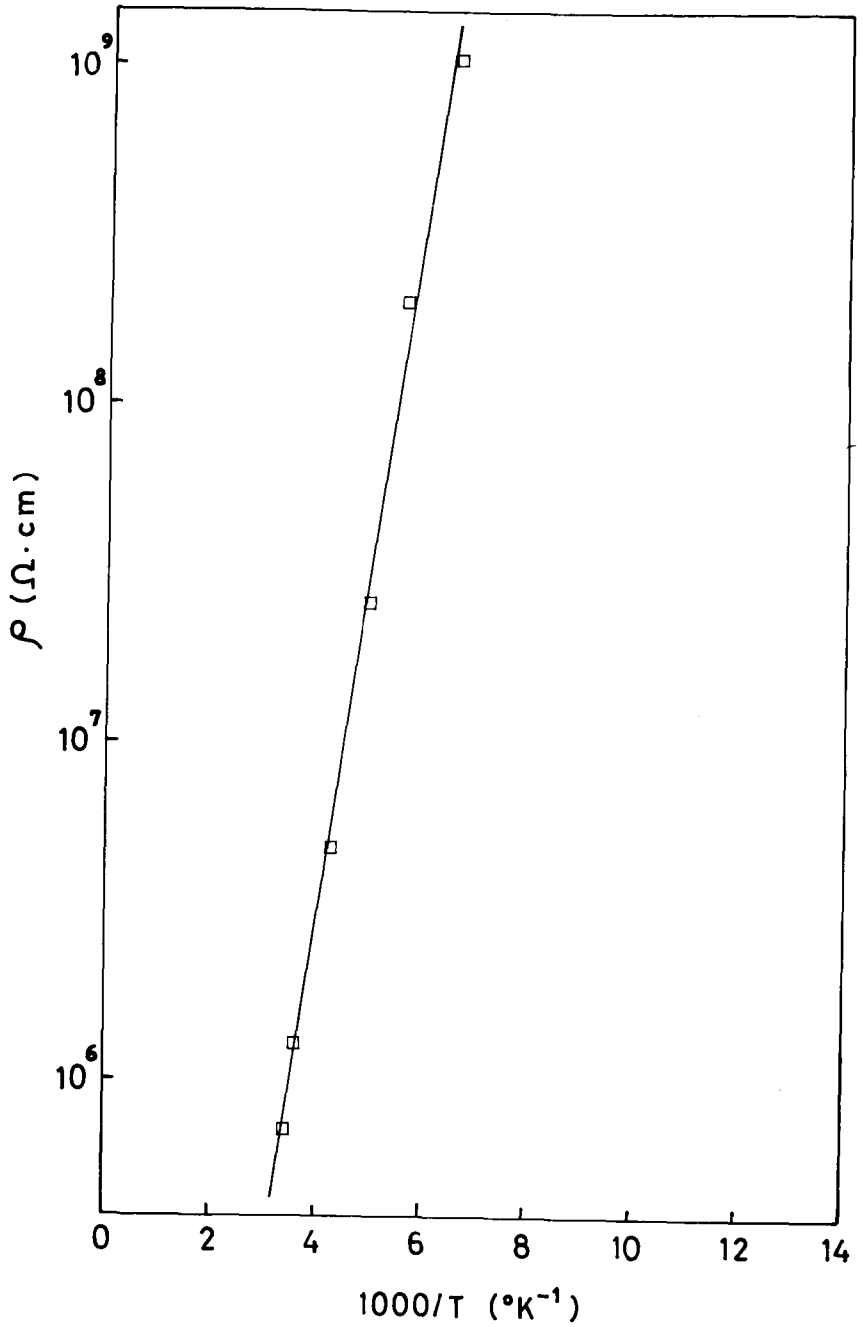

Fig. 27. Log. electrical resistivity of $(Ca_{0.4}Sr_{0.6})FeO_{2.58}$ vs. reciprocal temperature.

reveal that a-spacing of each composition tends to expand linearly with increasing oxygen deficiency, neglecting the abrupt behavior of the compositions with x = 0.2 and $(Ca_{0.4}Sr_{0.6})FeO_{2.77}$ and, an eventual tetragonal distortion takes place for the first time when the oxygen deficiency comes up to the composition $AFeO_{2.82}$ (64% Fe^{4+}). Furthermore, the data shown in Table I suggests that increasing concentration of oxygen vacancies leads to a precipitation of $SrFeO_{2.5}$ (a brownmillerite-like phase) as a second phase at the compositions less than 54% Fe^{4+}. These results are not far from those obtained by MacChesney et al. for the system $SrFeO_{2.5-3.0}$. They have found that $SrFeO_{2.72-3.00}$ (44-100% Fe^{4+}) are single-phase perovskites and increasing concentration of anion vacancies results in an expansion of the cubic lattice and a drastical tetragonal distortion is demonstrated at the compositions $SrFeO_{2.72-2.84}$ (44-68% Fe^{4+}). These phenomena may be explained in terms of the structural correlation between perovskite ($AFeO_3$) and dicalcium ferrite-like compound ($AFeO_{2.5}$). Wadsley[33] has pointed out their structural resembrance; in the case of $AFeO_{2.5}$ ($A_2Fe_2O_5$), where complete rows of oxygen atoms are regularly missing, and the accompanying movements of atoms remaining in the same planes, impose tetrahedral coordination upon the iron atoms, while in the case of $AFeO_3$, where the oxygen atoms are arranged to be cubic-close-packed together with the A atoms, all of the iron atoms occupy the resulting octahedral interstices, as indicated from Fig. 28. In other words, the dicalcium ferrite-like structure ($AFeO_{2.5}$) should be derived from the cubic perovskite ($AFeO_3$)structure by

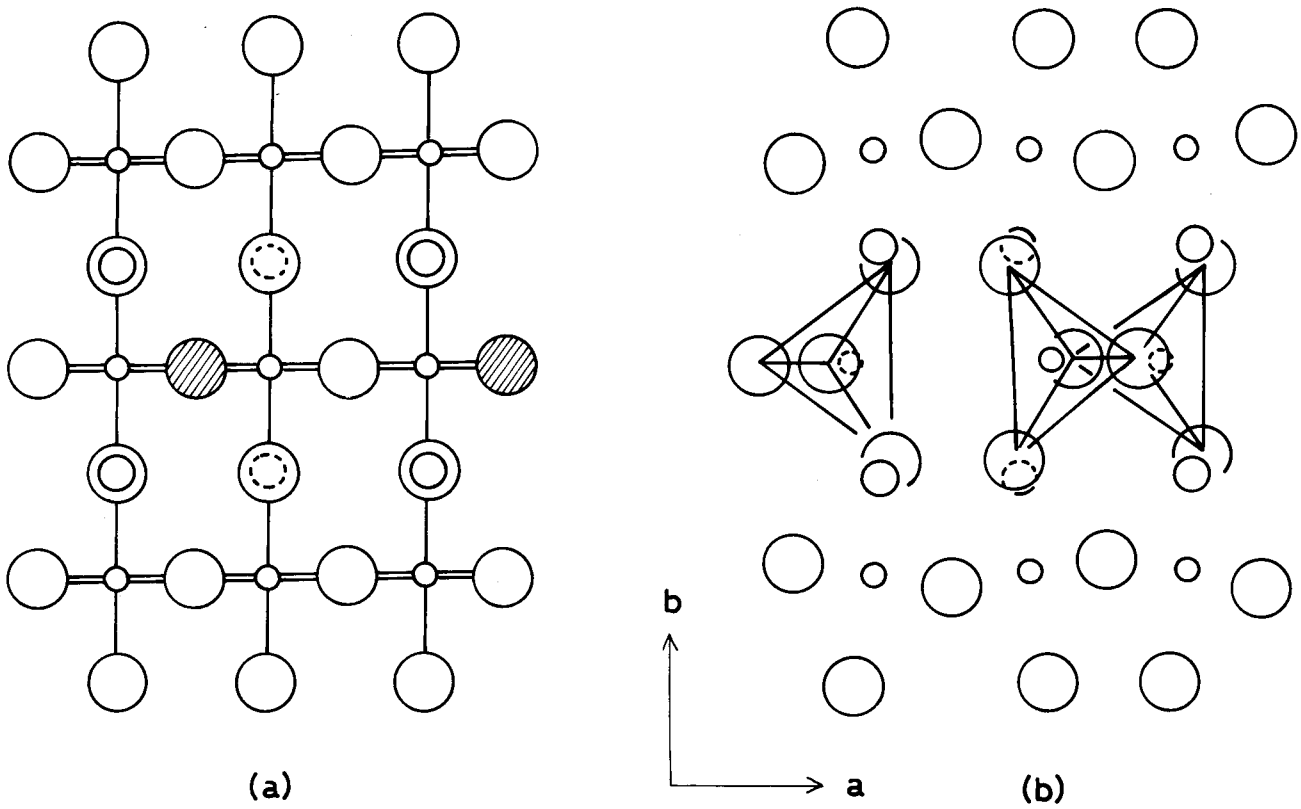

Fig. 28. Crystallographic relationship between (a) the perovskite structure ($AFeO_3$) projected on to (110) and (b) the brownmillerite-like structure ($A_2Fe_2O_5$ or $AFeO_{2.5}$): the largest circles refer to oxygen, intermediate ones A ions, and smallest the Fe ions. In $A_2Fe_2O_5$, oxygens (hatched circles) are missing from the central row of octahedra, in the perovskite lattice, the remainder regrouped into tetrahedra which are outlined.

regularly taking the oxygen atoms (shaded circles in Fig. 28 and 29), which are in a row in the (110) planes, away out of the latter lattice. Consequently, as oxygen vacancies are introduced in a cubic perovskite lattice, charge compensation is accomplished by converting the pair of iron ions sharing the vacancy to iron(III) ions, as has been reported by Gallagher et al.[10] A structural distortion is also induced in the vicinity of the oxygen vacancy which leads to a general expansion of the lattice. Further increasing anion vacancies may result in an eventual tetragonal distortion of the perovskite lattice at the very point when the anion defects are ordered in certain lattice planes. This presumed model is plausible for the present system $(Ca_xSr_{1-x})FeO_{3-\delta}$ $(0 \leqq x \leqq 0.4)$ studied.

Another important problem must here be discussed concerning the unsuccessful preparation of $CaFeO_3$ with the perovskite structure. The present high oxygen pressure technique failed to produce $CaFeO_3$(IV) in spite of the violent oxidation of $Ca_2Fe_2O_5$(III) at oxygen pressures up to ca. 1500 atm. In 1926, Goldschmidt[34] proposed a tolerence factor, t, which is a measure of the degree of misfit of perovskite structure. It can be defined by the equation

$$r_A + r_O = \sqrt{2}\, t(r_B + r_O),$$

where r_A, r_B, and r_O refer to the ionic radii of A, B, and O ions of the perovskite compound ABO_3, respectively. Using Pauling's ionic radii, any value of the tolerence factor for the known

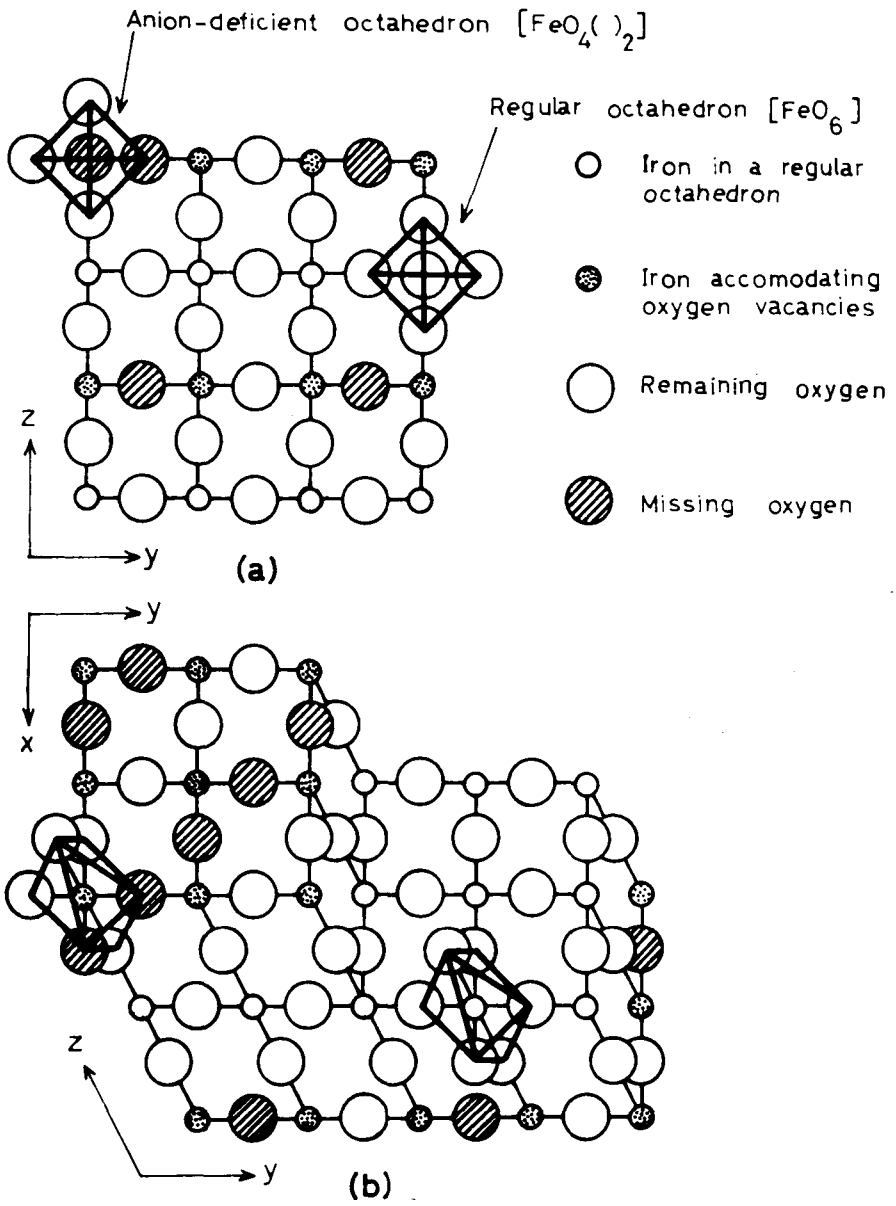

Fig. 29. Presumed oxygen-deficient perovskite with the composition $A[Fe]_{0.5}(Fe)_{0.5}O_{2.5}(\ )_{0.5}$: (a) the projection on to (100) and (b) the oblique projection on to (001), where [Fe] refers to the iron in the octahedral site, (Fe) the iron in the anion-deficient octahedral site, and ( ) the missing oxygen.

perovskites drop between 0.71 and 0.99.[35)-38)] Of the presumed isomorph of calcium ferrate ($CaFeO_3$), the estimated value is 0.89*. From this standpoint, it is not difficult to form a perovskite lattice with the composition $CaFeO_3$. It is subsequently deduced that calcium ferrate(IV) having the perovskite structure must be formed by intense oxidation of dicalcium ferrite(III) under an extremely high oxygen pressure (at least higher than an order of 10^4 atm).

2) ^{57}Fe Mössbauer effect

Isomer shift in iron compounds correlates with the valency state of the iron. Previous investigators have reported that the isomer shift for a chemically "bound" Fe^{4+} ion allocates the region between -0.19 mm/sec and +0.22 mm/sec (relative to 310 stainless steel). As for the present system, it is therefore natural to conclude that the dominant peak in the spectra for the perovskite compositions corresponds to the Fe^{4+} state. The spectra for near-stoichiometric perovskites, $SrFeO_{2.98}$ and $(Ca_{0.2}Sr_{0.8})FeO_{2.99}$, are presented in Figs. 11 and 12. The values of the isomer shift are much less negative than that predicted by elementary theoretical calculations[40)] based on a purely ionic $3d^4$ configuration. As reported earlier,[41)] the isomer shift of potassium ferrate(VI) is also small of that predicted. As the charge of the iron ion increases and its redius decreases, the bonding becomes undoubtedly

---

* For this calculation, the value of 0.58Å[39)] was used as the radius of Fe^{4+} ion.

more covalent due to the increased polarization of the surrounding oxygen atoms. The contribution of electron density or charge from the covalent bonding may induce an isomer shift in either direction from the purely ionic value depending upon whether it adds predominantly to the inner 3d level or the outer 4s level. An additional s-electron component would result in a higher charge density at the nucleus, while an enhancement of the 3d electron density provides greater screening of the s electrons and, consequently, a reduced charge density at the nucleus. The latter appears to be true for compounds of the higher valency states of iron.

The isomer shifts of both Fe^{4+} and Fe^{3+} ions for the system $(Ca_xSr_{1-x})FeO_{3-\delta}$ ($0 \leqq x \leqq 0.6$; $0.01 \leqq \delta \leqq 0.19$) are plotted as a function of Fe^{4+} concentration in Fig. 30. First the figure implies that the isomer shift of Fe^{4+} increases slightly and that of Fe^{3+} dereases as the perovskite-phase composition approaches a stoichiometric one. Such phenomena have been observed for $SrFeO_{2.5-3.0}$,[10] $La_{1-x}Sr_xFeO_3$,[11] and $Sr_3Fe_2O_{6-7}$.[42] it is deduced therefrom that an increase in oxygen fraction results in the covalent contribution of the anions to the 3d level of iron(IV), whereas oxidation process may make iron(III) transfer to iron(IV), followed by the removal of an electron from the 3d shell of iron(III). Such a covalent contribution based on a collupse of anion vacancies seems to be consistent with the lattice contraction measured by X-ray diffractometry.

Secondary, the results presented in Fig. 30 strongly demonstrates a sudden change in isomer shift at the composition with 62% Fe^{4+}. As seen in Figs. 11-14, the spectra of the composition

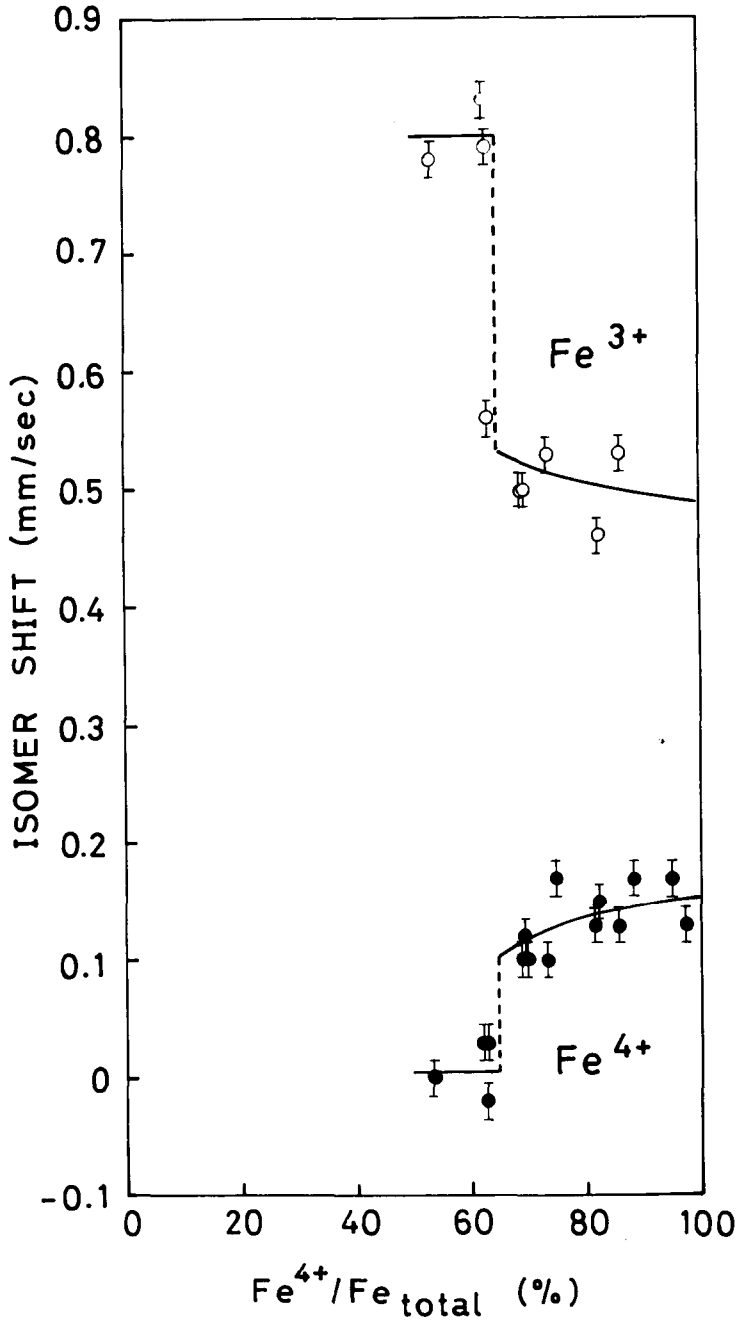

Fig. 30. Isomer shift vs. the ratio Fe^{4+}/Fe_{total} for both Fe^{3+} and Fe^{4+} ions in the system $(Ca_xSr_{1-x})FeO_{3-\delta}$.

with the Fe^{4+} contents less than 62% display sizable quadrupole splittings for both Fe^{4+} and Fe^{3+} resonances. The average quadrupole-coupling evergies are 0.29 and 0.50 mm/sec, respectively. This seems to be in contradiction to the electronic configurations of both Fe^{4+} and Fe^{3+} ions, i.e., $3d^4$ ($^5D_0$) and $3d^5$ ($^6S_{5/2}$), respectively, since quadrupole interaction is generally greater for a one-electron-vacancy ion (Fe^{4+}) than for a spherical ion (Fe^{3+}). As mentioned before, in the stoichiometric iron(IV) compounds with the perovskite structure the iron ions are surrounded by a regular octahedron of oxygen ions and each oxygen ion is shared by two iron ions. Concludingly, the reason why the quadrupole splitting energy of the iron(III) is much larger than that of the iron(IV) is explained in terms of the local asymmetric ligand field at the iron(III) nucleus.

3) Magnetic and electric properties

From the paramagnetic measurements, the molar effective magnetic moments were calculated for the perovskites $(Ca_xSr_{1-x})FeO_{3-\delta}$ ($0 \leqq x \leqq 0.6$; $0.01 \leqq \delta \leqq 0.19$) by using the equation

$$\mu_{eff} = \sqrt{\frac{3k}{N\beta^2}\chi_m(T-\theta)}$$

$$= 2.83\sqrt{C_m},$$

where μ_{eff} is the moment per molecule in Bohr magnetons, k the Boltzman's constant, N the Avogadro's number, β a Bohr magneton, χ_m the molar susceptibility, T the temperature in degrees Kelvin, θ the paramagnetic Curie temperature and C_m the molar Curie

constant. The estimated moments* are plotted as a function of Fe^{4+} concentration in Fig. 31. As for the perovskites with a higher oxygen fraction, the effective moments are abruptly larger than the theoretical values estimated by using a high-spin model. Such an abrupt characteristic has been observed for the system $SrFeO_{3-\delta}$ by MacChesney et al.[3)]

Another interesting phenomenon was found for the magnetic properties of the system studied; that is, a maximum is observed in the plots of μ_{eff} vs. Fe^{4+} concentration at the composition around 95% Fe^{4+}. Such a feature has been also seen in the results obtained by MacChesney et al.[3)] (see Fig. 32). This unique evidence is not adequately explained, but it seems to be essential that strontium ferrate with the perovskite structure is a high-spin compound. The present system is composed of cubic or slightly distorted perovskites which are thought to be essentially antiferromagnetic at lower temperatures from the curves of $1/\chi_m$ vs. T. Nevertheless, almost all of the specimens take "positive" paramagnetic Curie temperatures implying a ferromagnetic interaction (see Fig. 33). The positive exchange integral of the near-stoichiometric compounds suggests that the materials are not G-type compounds.

The electrical resistivity investigated for the perovskites of the system $(Ca_xSr_{1-x})FeO_{3-\delta}(0 \leqq x \leqq 0.6)$ tends to be temperature-independent with the decrease of oxygen deficiency and

---

* The maximum error is ±0.15 Bohr magnetons.

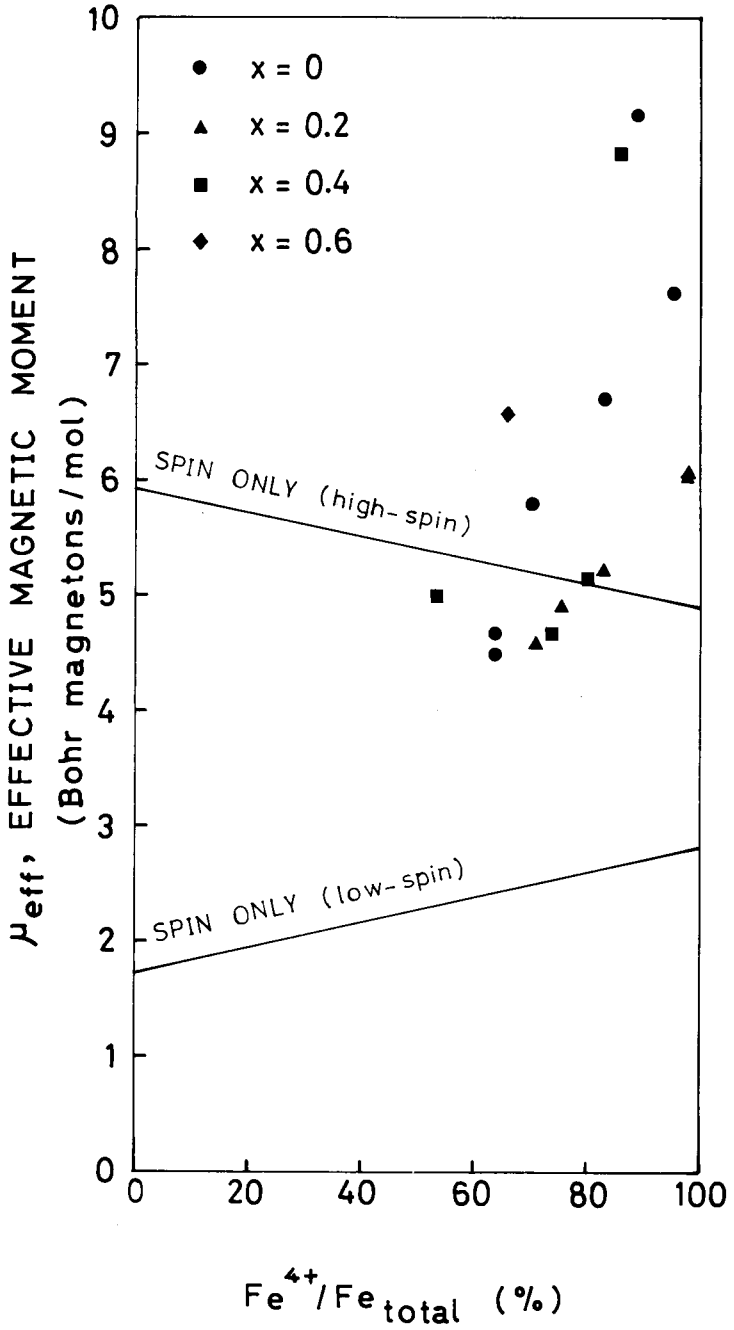

Fig. 31. Effective magnetic moment vs. the ratio Fe^{4+}/Fe_{total} for the system $(Ca_xSr_{1-x})FeO_{3-\delta}$.

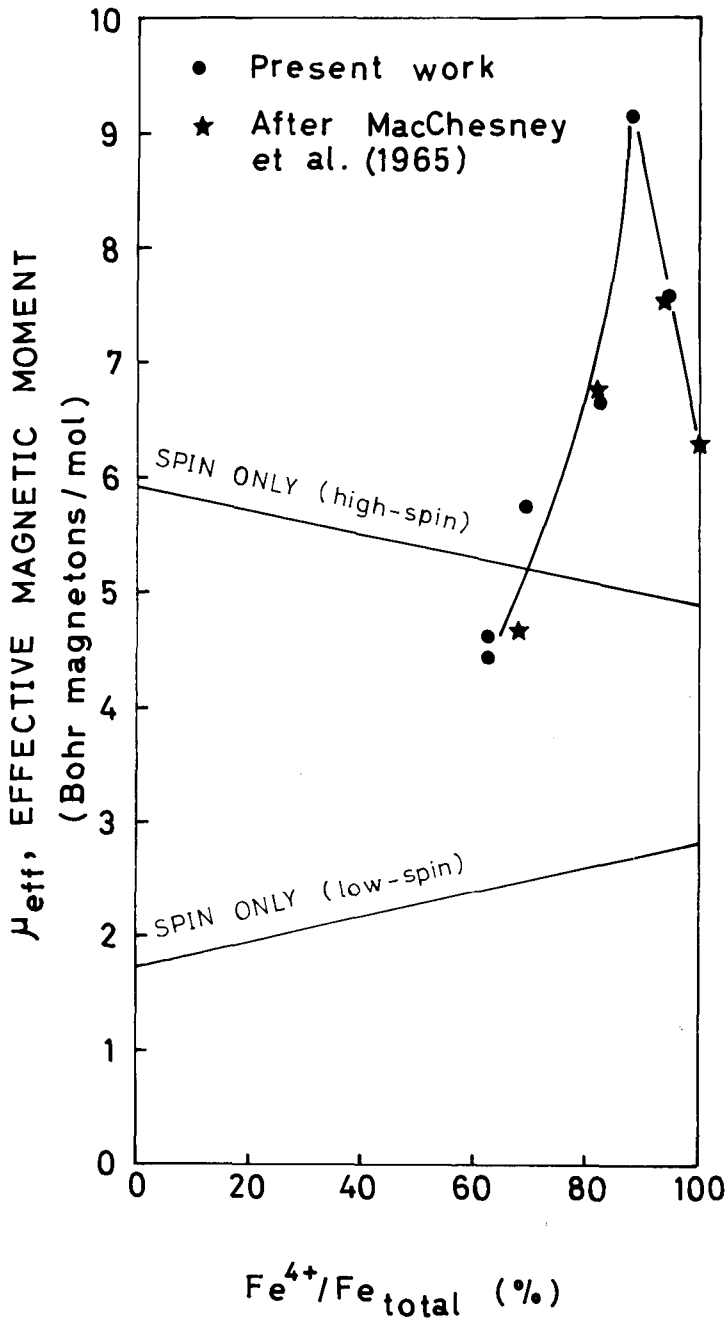

Fig. 32. Effective magnetic moment for strontium ferrate compositions of different Fe^{4+} contents.

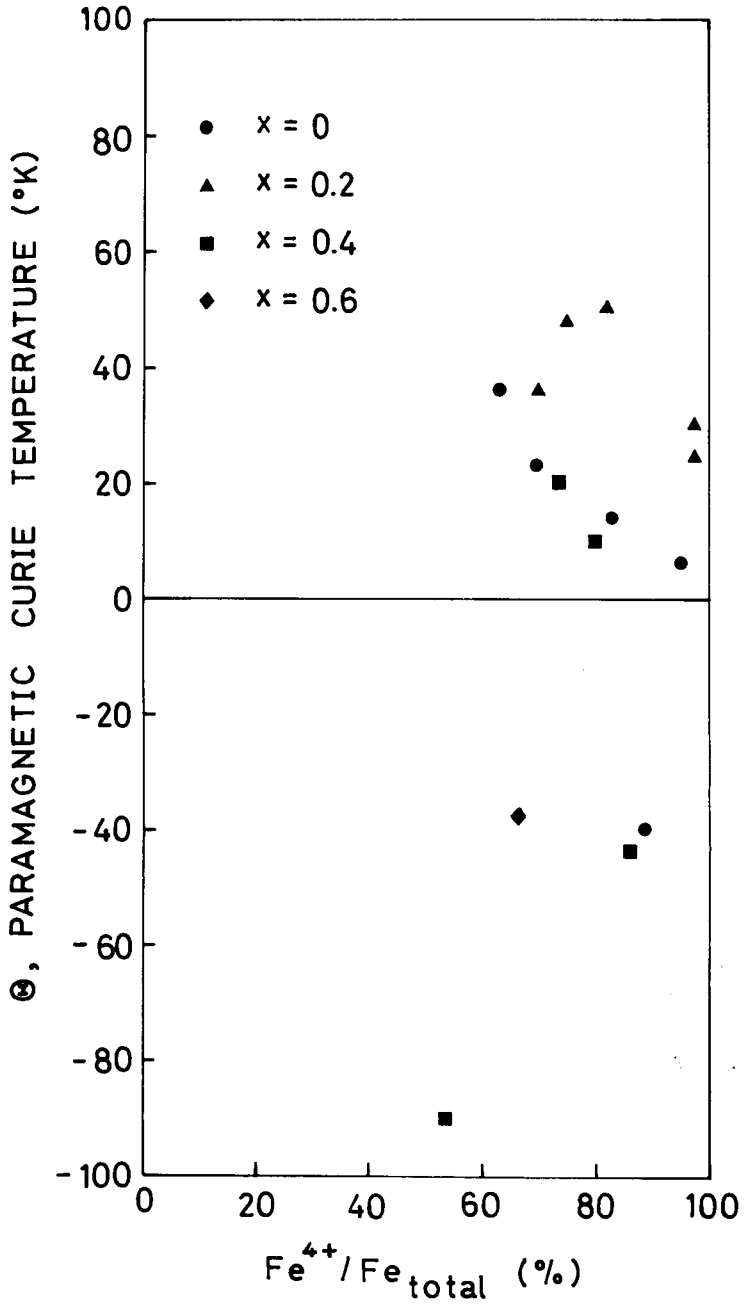

Fig. 33. Paramagnetic Curie temperature vs. the ratio Fe^{4+}/Fe_{total} for the system $(Ca_xSr_{1-x})FeO_{3-\delta}$.

temperature. MacChesney et al.[3] have also reported the nearly zero activation energies for the Fe^{4+}-rich perovskites, $SrFeO_{2.84-3.00}$, below their Néel temperatures; particularly, the stoichiometric composition has shows a zero activation energy over the whole temperature range studied, i.e., 4.2°K to 300°K.

Electrical conduction of strontium ferrate has been discussed previously in connection with investigations of the lanthanum-strontium ferrates.[8] Here, the rather high conductivity was explained according to the electron-hopping mechanism by de Boer and Verway.[43] In accord with the behavior of ionic oxides, it was proposed that transition-metal oxides in which the transition-metal is in one valence state only are insulators. Nevertheless, near-stoichiometric strontium ferrates with the perovskite structure examined by MacChesney et al.[3] and the present author exhibited properties quite different from those anticipated. Furthermore, Gallagher et al.[10] have measured the X-ray reflections of $SrFeO_{3.00}$ at the temperatures of 4.2°K and 299°K. Close scrutiny of the diffraction patterns failed to reveal Jahn-Teller distortion.

As pointed out by MacChesney et al.[12] and Goodenough,[44] it is likely that $SrFeO_3$ is transitional between the localized and collective electron situations, for although it is a metallic conductor and does not show Jahn-Teller distortion, it appears magnetically ordered at low temperatures. The more positive isomer shift of $SrFeO_3$ than that predicted for purely ionic Fe^{4+} has implied a significant covalent mixing of anion p and cation

d orbitals. Such a covalency makes the molecular orbital theory apply for the system where the molecular orbitals composed of both antibonding π^* (a mixing of t_{2g} and p_π) and Σ^* (amixing of e_g and p_σ) orbitals are formed. Moreover, if a certain band formation is allowed for the Σ^* orbitals in the strontium ferrate crystal because of the three-dimentional covalent framework, such an electron occupying the Σ^* band is no longer localized but collective enough to behave as a metallic one, whereas three electrons in each of the π^* states remain localized as magnetic spins. From this standpoint, the semi-metallic conduction, temperature-dependent paramagnetic behavior and the absence of Jahn-Teller distortion of strontium ferrate(IV) seems to be reasonably explained despite the large degeneracy anticipated for the Fe^{4+} ion, which, if in the high spin state, would have the electronic configuration $3d_{t_{2g}}\ 3e_g1$. Recently a rare perovskite with the composition $SrCrO_3$ has been prepared using a tetrahedral anvil at high pressures.[45] The measurements of electric and magnetic properties revealed that this material is also metallic. However, the conduction mechanism of $SrFeO_3$ is thought to be quite different from those of $SrCrO_3$ and $LaNiO_3$[46] which show Pauli paramagnetism, though these three materials are all perovskites.

Therefore, it is concluded that the electrical conduction of the perovskite compositions in the present system is explained by similar mechanism proposed by MacChesney and others; i.e. these materials are classified into the magnetic semiconductors whose characteristics are caused by their unique bond nature. It is also

elucidated that as the oxygen atoms are taken off from a perovskite lattice and the chemical composition approaches to that of the brownmillerite-like structure, its electrical properties changes from semimetallic to semiconductive or insulative. This behavior is also explained in terms of the difference in bond nature between the perovskite and the brownmillerite-like structure, i.e., covalency and ionicity.

Chapter 3

A New Perovskite $CaFeO_3$(IV)

The studies of high oxygen pressure effect in the system $(Ca_xSr_{1-x})FeO_{3-\delta}$ $(0 \leqq x \leqq 1)$, described in chapter 2, revealed that the formation of perovskite-like compounds was limited to the composition range from x = 0 to x = 0.8 at oxygen pressures up to ca. 2000 atm. As for calcium ferrate(IV) with the perovskite structure, it has been predicted to synthesize the material at a much higher oxygen pressure. For the increase of the fugasity of oxygen gas in a reactor, it is desirable to make use of the dissociative oxygen pressure of higher-valency oxides, peroxides and superoxides. Among these, chromium trioxide has been extensively studied[47)-50)] for the correlation with other chromium-oxygen system from the thermodynamic point of view. As seen from Fig. 34, chromium trioxide(VI) equilibrates with chromium dioxide(IV) at 20-25 Kb and 1000-12000 °C:

$$CrO_3 \rightleftharpoons CrO_2 + 1/2\ O_2.$$

Therefore, it seems to be possible to generate an oxygen pressure of the order of 10^4 atm, finding the adequate pressure-temperature conditions at which the reactant-resultant system is completely brought to the right-hand side of the above equation. In such a way, liberated oxygens from the decomposition of chromium trioxide will be used to prepare calcium ferrate(IV) with the perovskite structure.

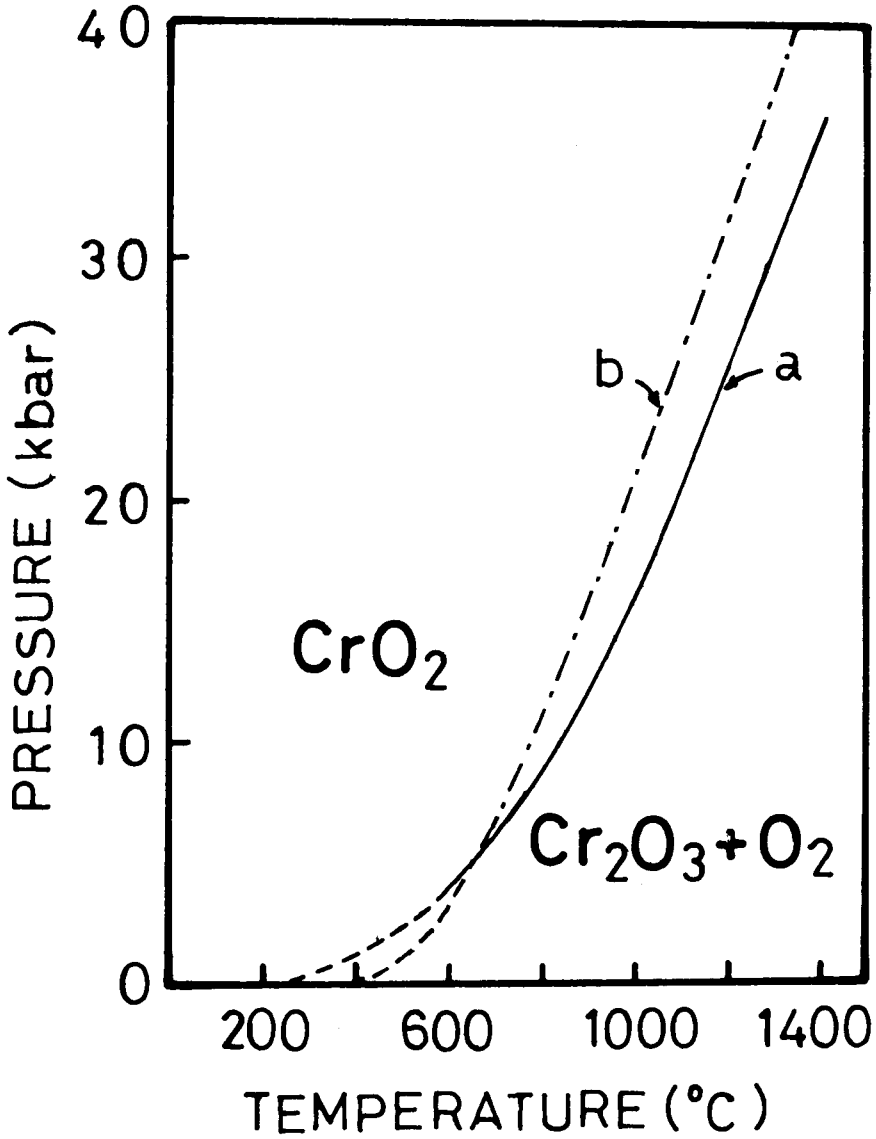

Fig. 34. Pressure vs. temperature equilibrium diagram for the system CrO_2-Cr_2O_3 after (a): Fukunaga et al.[49] and (b): DeVries.[50]

In this chapter, the author describes the fruitful preparation of a new perovskite $CaFeO_3$ using a piston-sylinder-type high-pressure-vessel and also CrO_3 as an oxidizing agent.

EXPERIMENTAL PROCEDURES

A starting material with the composition $Ca_2Fe_2O_5$, which has been prepared by firing of an intimate mixture of $CaCO_3$ and Fe_2O_3 at 1200 °C, was put together with dry CrO_3 into a gold-tube capsule. A zirconium dioxide layer was intervened between the two layers composed of $Ca_2Fe_2O_5$ and CrO_3 in order to preclude the product from any undesirable contamination with CrO_3, as shown in Fig. 35. The capsule was then pressed in a piston-cylinder-type high-pressure-vessel at 20-25 Kb and 900-1100 °C* for 1 hr. Cooling of the sample was conducted under the pressed condition.

To check whether or not the product is a perovskite phase, some physico-chemical properties were examined, based on X-ray diffractometry, Mössbauer spectroscopy and magnetic measurements. Contamination of the resulting material with zirconium and chromium was examined by qualitative colorimetry using Alizarin Red S (sodium alizarinsulfonate)[51] and diphenylcarbazide,[52] respectively.

---

*The pressure-temperature conditions are those at which CrO_2 is thermodynamically more stable than CrO_3.

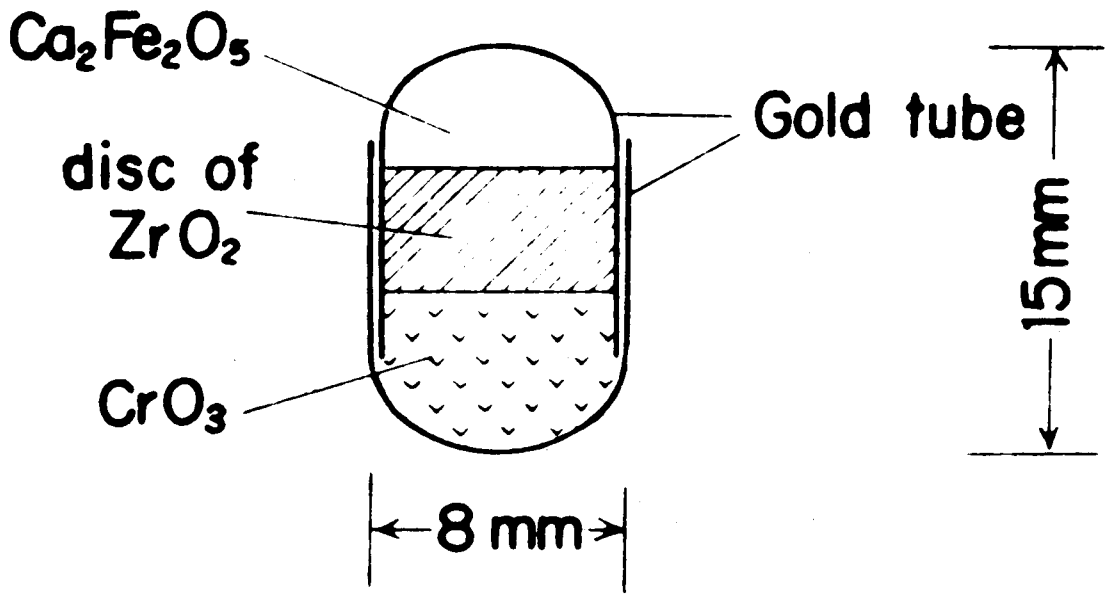

Fig. 35. Sandwich-type cell consisted of a starting material $Ca_2Fe_2O_5$, a disk of ZrO_2 intervened for the protection against contamination of a sample with CrO_3, and dry CrO_3 as an oxygen source.

EXPERIMENTAL RESULTS

The X-ray diffractogram of calcium ferrate(IV) prepared through this technique is shown in Fig. 36. All of the reflections were indexed as those of a cubic perovskite-like compound, whereas the starting material $Ca_2Fe_2O_5$ had an orthorhombic brownmillerite-like structure. The lattice parameter of calcium ferrate(IV) varies with the mixing ratio of $Ca_2Fe_2O_5$ to CrO_3 in weight. For example, the a-spacing of calcium ferrate(IV) was 3.798 Å at the ratio of 2/3, while that was 3.770 Å at the ratio of 1/2.

Figure 37 shows the ^{57}Fe Mössbauer spectra of calcium ferrates(IV) prepared at varying ratio of $Ca_2Fe_2O_5/CrO_3$; i.e., spectrum A is of the ratio of 1/2 and spectrum B of 2/3. Either spectrum exhibits a paramagnetic Fe^{4+} absorption (IS = +0.13 mm/sec) implying the formation of a perovskite phase of calcium ferrate, though spectrum B shows an additional Fe^{3+} absorption (IS = +0.80 mm/sec) corresponding to anion vacancies. In chapter 2, it was described that oxygen deficiency results in the expansion of a-axis for non-stoichiometric perovskites. Such effect may also be taken in account for the calcium ferrates just prepared in this work. Since the lattice parameter of sample A is smaller than that of sample B, the former sample seems to be a near-stoichiometric perovskite and the latter may have appreciable oxygen vacancies. This inference is not far from the results presented in Fig. 37.

Next magnetic susceptibilities were measured for the two

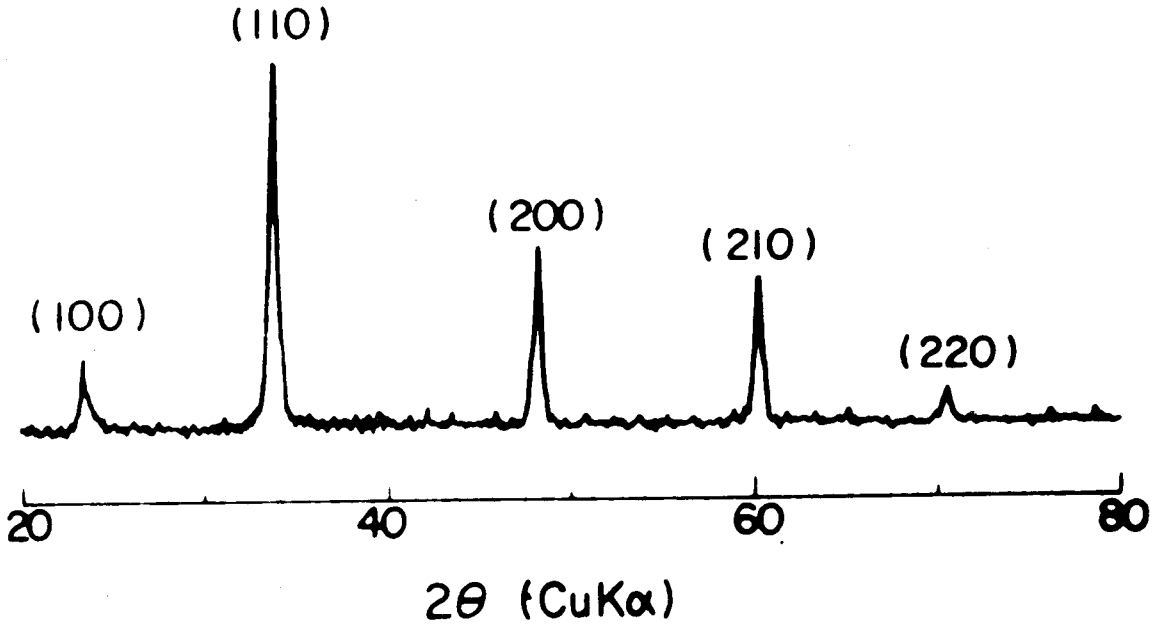

Fig. 36. X-ray diffractogram of calcium ferrate with the cubic perovskite structure.

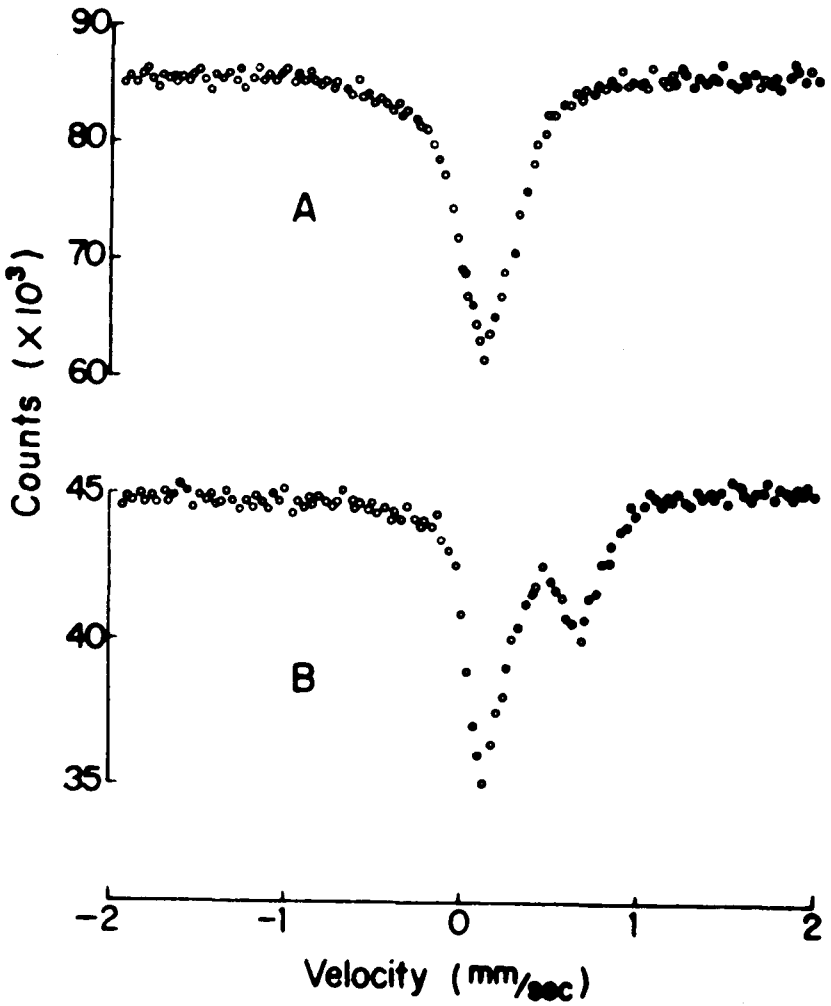

Fig. 37. Mössbauer spectra for calcium ferrates with the cubic perovskite structure: A is that of a sample with a_o = 3.770 Å and B of a sample with a_o = 3.798 Å.

compositions. The inverse of susceptibility is plotted in Fig. 38 as a function of temperature. Either specimen is antiferromagnetic, having a Néel temperature around 120 °K. For sample A, the paramagnetic Curie temperature is 78 °K and the effective magnetic moment is 2.20 Bohr magnetons per mole. On the other hand, sample B has a Curie temperature of 45 °K and an effective magnetic moment of 2.71 Bohr magnetons per mole.

Any significant contamination of the resulting perovskite-like compounds with zirconium and chromium was not observed.

DISCUSSIONS

Calcium ferrate(IV) with the cubic perovskite structure, which had not yet been synthesized for a long time, has just prepared in this work. As a preliminary work, the author intended to prepare $CaFeO_3$(IV) in a piston-cylinder-type high-pressure-vessel without CrO_3. The attempt, however, failed as expected. Therefore, it is concluded that calcium ferrate(IV) should be produced only at an effective oxygen pressure generated by the decomposition of chromium trioxide, such as

$$1/2\ CrO_3(VI) \xrightarrow[900\text{-}1100\ ^\circ C]{20\text{-}25\ Kb} 1/2\ CrO_2(IV) + 1/2\ O_2$$

$$Ca_2Fe_2O_5(III) + 1/2\ O_2 \longrightarrow 2\ CaFeO_3(IV).$$

From the reaction formula just above, the preparation of a stoichiometric calcium ferrate(IV) requires a half mole of CrO_3 for every mole of the starting material $Ca_2Fe_2O_5$. In this experiment, a near-stoichiometric $CaFeO_3$(IV) has been prepared under the con-

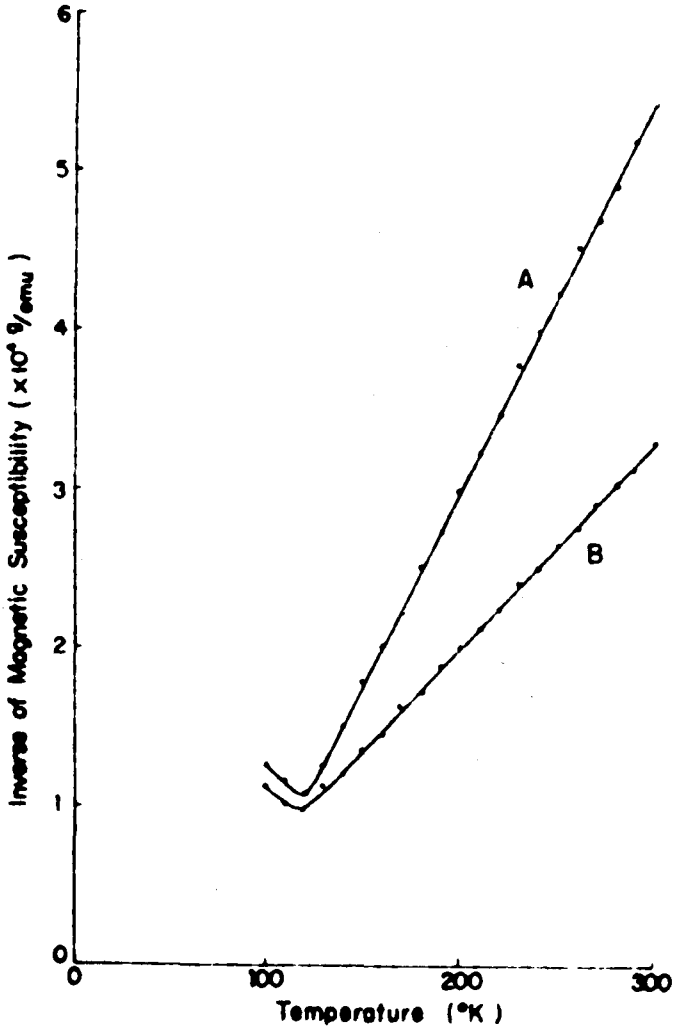

Fig. 38. Reciprocal magnetic susceptibility vs. temperature for calcium ferrates with the cubic perovskite structure: A is that of a sample with a_o = 3.770 Å and B of a sample with a_o = 3.798 Å.

dition of the ratio $Ca_2Fe_2O_5/CrO_3$ of 1/2 in weight. Therefore, excess oxygens are necessary to promote the complete reaction:

$$Ca_2Fe_2O_5(III) + 1/2\ O_2 \longrightarrow 2\ CaFeO_3(IV).$$

The present results suggest that a high oxygen pressure far above an order of 10^3 atm is obtained through this technique, and such a unique technique seems to be very useful for the preparation of similar compounds containing a transition metal ion in the abnormally higher valence state.

Here, it is worthwhile to mention briefly the physico-chemical properties measured by X-ray diffractometry, ^{57}Fe Mössbauer spectroscopy and magnetometry for the near-stoichiometric calcium ferrate(IV) so prepared.

First, one can not recognize any significant difference in the isomer shift of iron(IV) between the two extreme compositions, $SrFeO_3$ and $CaFeO_3$, in the present system studied, i.e., their isomer shifts are almost same within the present experimental error of ± 0.03 mm/sec. Furthermore, those isomer shifts are compatible with those of near-stoichiometric $(Ca_xSr_{1-x})FeO_{3-\delta}$ ($x = 0.2$ and $x = 0.4$). Subsequently, it is concluded that any measurable difference in isomer shift is not between calcium and strontium ferrates(IV), despite of their different lattice dimensions.

One other interesting phenomenon was found in the measurement of magnetic susceptibility of a near-stoichiometric $CaFeO_3$ (IV); it demonstrates a unique behavior, different from that of the system $(Ca_xSr_{1-x})FeO_{3-\delta}$ ($0 \leqq x \leqq 0.6$). The effective magnetic moment found for this material was 2.20 Bohr magnetons per mole,

though strontium-rich perovskites had an abruptly larger Bohr magneton than that predicted for the system using a high-spin model. The very low moment of $CaFeO_3$(IV) undoubtedly indicates that the material is either a low-spin compound or such a compound as the bonding nature of iron-oxygen octahedron is a $d_\gamma^2sp^3$ hybrid. Such a difference in electronic configuration of iron(IV) between the two compounds seems to be explained in terms of the ligand field strength of oxygen atom correlating with cation-anion separation. In order to examine the validity for this model, the magnetic susceptibility was measured also for a near-stoichiometric perovskite $(Ca_{0.8}Sr_{0.2})FeO_3$ with a smaller cell volume. This material, which was synthesized at 20 Kb and 1100 °C for 1 hr in a piston-cylinder-type high-pressure-vessel using CrO_3 as an oxygen source, exhibited a smaller effective Bohr magneton of 3.67 and a cell constant of a_o = 3.793 Å. Therefore, it is concluded that the electronic configuration of iron(IV) of the present system $(Ca_xSr_{1-x})FeO_{3-\delta}$ with the perovskite structure changes from a high-spin to low-spin state at the composition with x = ca. 0.8 and a_o = ca. 3.80.

Chapter 4

Summary

This paper has described a high oxygen pressure effect in the system $(Ca_xSr_{1-x})FeO_{3-\delta}$. Such a system is of unique interest in that it exhibits a wide range of oxygen non-stoichiometry, as well as in that it contains an unusual "Fe^{4+}" ion. Moreover, the a-long-time pending problem why normal solid-state reaction does not yield calcium ferrate(IV) with the perovskite structure while the strontium analog and calcium titanate(IV) are known, encouraged the author to undertake the present study.

For the purpose, a series of materials with the composition $(Ca_xSr_{1-x})FeO_{3-\delta}$($0 \leqq x \leqq 1$, with x in the steps of 0.2 mole; $0.19 \leqq \delta \leqq 0.5$) was first prepared in air and the starting materials were next equilibrated at various oxygen pressures up to ca. 2000 atm and the temperatures ranging from 300 to 800 °C. The physico-chemical properties of these compositions with varying oxygen fraction were examined based upon X-ray diffractometry, ^{57}Mössbauer spectroscopy, magnetometry and electrical measurement. The X-ray analysis clarified that a cubic perovskite phase is stabilized at the composition range $AFeO_{2.82-3.00}$ ($Fe^{4+} \geqq 64\%$), a tetragonal distortion appears at the composition with the Fe^{4+} contents less than 62%, and composition with the Fe^{4+} contents between 0% and 54% undergo a precipitation of $A_2Fe_2O_5$ with the brownmillerite structure. As for perovskite

phase, the a-spacing showed a linear expansion with increasing anion deficiency, whereas the c-spacing of a tetragonal perovskite phase does not change but remains nearly comparable to the a-spacing of the corresponding stoichiometric perovskite phase. The characteristic behavior has been explained in terms of a short-range ordering of missing oxygens since close scrutiny of the diffraction patterns of anion-deficient perovskites exposed on a Guinier camera failed to find any additional superstructural lines. One other important result has been obtained; the present high oxygen pressure technique described in detail in chapter 2 was unable to oxidize dicalcium ferrite up to the iron(IV)-bearing perovskite composition but made the formation of perovskite phase limited to the composition of x = 0.8.

Iron-57 Mössbauer measurements presented the results as follows: (1) a near-stoichiometric perovskite showed a single paramagnetic Fe^{4+} resonance absorption, whose isomer shift (+ 0.15$\pm$0.02 mm/sec relative to 310 stainless steel at room temperature) was more positive than that anticipated for a "free" ionic Fe^{4+} (-1.30mm/sec). The discrepancy was interpreted in terms of the covalent contribution of anions to the 3d levels of the "bound" iron(IV). (2) As predicted from the results obtained by X-ray diffractometry, a tetragonal perovskite demonstrated sizable Quadrupole couplings for both Fe^{4+} and Fe^{3+} nuclei. However, their coupling energies were quite strange when only their electronic configuratons were taken for the irons into accounts, because the iron(III) has a spherical configuration whereas the iron

(IV) has a one-electron-vacant half-filled 3d shell. Nevertheless, the larger energy for the iron(III) was explained in terms of the localized vacancies contiguous to the iron(III). (3) There was not a great difference among the isomer shifts of cubic perovskites, while an introduction of a number of oxygen vacancies in the perovskite lattice resulted in a sudden change in isomer shift, corresponding to the X-ray tetragonal distortion. This might also be explained in terms of covalency and ionicity.

Here, the magnetic and electric measurements of the system $(Ca_xSr_{1-x})FeO_{3-\delta}(0 \leqq x \leqq 0.6)$ discussed in chapter 2, are summarized as follows: (1) iron(IV)-rich compositions displayed an abruptly high effective magnetic moment, far higher than that predicted using a high-spin model. Particularly, the compositions with the Fe^{4+} contents around 87% showed a muximum in the plots of μ_{eff} as a function of Fe^{4+} concentration, consisting to the negative paramagnetic Curie temperature. These unique phenomena have not understood adequately. (2) As for the system $SrFeO_{2.81-2.98}$, the almost stoichiometric composition had a Néel temperature of 115 °K, whereas the more anion-deficient showed a decreasing Néel temperature as oxygen vacancies were induced in the lattice. The characteristic feature seems to be explained as such that the antiferromagnetic spin alignment of Fe^{4+}-Fe^{4+} via superexchange mechanism involving the intervening oxygen is undubtedly perturbed as a consequence of the presumed oxygen vacancies and the resulting lattice expansion. (3) Semiquantitative measurements of electrical resistivity using a two-probe method

showed that a nearly temperature-independent conduction appeared in the system with a high Fe^{4+} concentration at the temperature range where an antiferromagnetic ordering takes place, whereas the iron(III)-rich sample exhibited a typical semiconduction. Such an unexpected decrease in resistivity as the composion approachs $AFeO_3$(IV) is considered to be due to the formation of anti-bonding Σ^* band made up of the e_g orbitals of the 3d cations and the p_σ orbitals of the anions.

Finally, the author will summarize in brief the results reported for a new perovskite $CaFeO_3$(IV) in chapter 3. From the high oxygen pressure experiments examined for the system with the composition $(Ca_xSr_{1-x})FeO_{3-\delta}$, it has been much anticipated that a new perovskite $CaFeO_3$(IV) should be produced at a high oxygen pressure much above an order of 10^3 atm. For the aim at the preparation of the presumed perovskite, the author devised an effective oxidation technique in order to generate a much higher oxygen pressure than those obtained in the previous work. The procedure was as follows: excess dry chromium trioxide was bedded at the bottom of a gold-tube capsule as a source of available oxygens, and then a starting material with the chemical composition $Ca_2Fe_2O_5$ was sedimented on a CrO_3 layer, with a zirconium dioxide layer intervening between the CrO_3 and $Ca_2Fe_2O_5$ layers. The capsule subsequently embedded in a piston-cylinder-type high-pressure-vessel and pressed under the pressures ranging from 20 Kb to 25 Kb at 900-1100 °C for 1 hr. The resulting product was identified as the presumed isomorph of calcium titanate(IV), based

upon X-ray diffractometry. When the mixing ratio of $Ca_2Fe_2O_5$ to CrO_3 was 1/2 in weight, the lattice parameter found for the product was a_o = 3.770 Å, which was in good agreement with that extrapolated from the plots of the lattice parameters of the system $(Ca_xSr_{1-x})FeO_{3-\delta}$ $(0 \leq x \leq 0.4)$ vs. Fe^{4+} concentration.

Mössbauer spectroscopy also confirmed that the material $CaFeO_3$ so prepared was a paramagnetic (at room temperature) perovskite containing Fe^{4+} ions (IS = +0.13 mm/sec) as a major component. The isomer shift was comparable to that of strontium ferrate(IV) within the present experimental error of $\pm$0.03 mm/sec. However, the magnetic behavior of calcium ferrate(IV) was different from the strontium-rich compositions in the system $CaFeO_3$-$SrFeO_3$; the effective magnetic moment was 2.20 Bohr magnetons per mole for $CaFeO_3$(IV). Concludingly, it has been assumed that the material is a low-spin compound.

Moreover, from the experimental results for the magnetic susceptibility and lattice parameter of $(Ca_{0.8}Sr_{0.2})FeO_3$, it is clarified that the present system $(Ca_xSr_{1-x})FeO_3$(IV) is classified into two groups: high-spin compounds and low-spin compounds. There is the borderline between the two electronic states at the composition with $x \approx 0.8$ and the lattice constant of $a_o \approx 3.80$ Å.

Finally, calculations of the ionic radii of Fe^{4+} in the two different electronic states from the lattice parameters for two ultimate compositions, i.e., a high-spin strontium ferrate(IV) and a low-spin calcium ferrate(IV), were carried out and the results are as follows:

cation	coordination number	electronic state	ionic radius*
Fe^{4+}	6	high-spin	0.52_4 Å
Fe^{4+}	6	low-spin	0.48_5 Å

*Calculations are based on the Pauling's ionic radius of a six-fold coordinated oxygen divalent-anion.

Acknowledgments

The author is paticularly grateful to Assistant Professor S. Udagawa of Tokyo Institute of Technology for suggesting the problem and for helpful discussions during the cource of the investigation.

Thanks are also due to Professor M. Koizumi and Assistant Professor F. Kanamaru of the Institute of Scientific and Industrial Research, Osaka University, and also to Professor S. Kume of College of General Education, Osaka University, who encouraged and provided the author valuable suggestions in connection with this work.

The author is indebted to Professor R. Kiriyama and Professor N. Morimoto of the Institute of Scientific and Industrial Research, Osaka University, and also Professor S. Ikeda of Fuculty of Science, Osaka University for many useful suggestions and discussions in writing the present paper.

The author would like to thank Assistant Professor S. Kawai, M. Shimada, H. Miyamoto, Y. Shibasaki and Y. Mimura of Osaka University, and Professor T. Takada and Dr. T. Shinjo of Kyoto University, and Dr. Hirota of Research Laboratory, Wireless Division, Matsushita Electric Industrial Co. Ltd., and Professor S. Nomura, Professor S. Kawakubo, S. Igarashi, T. Hatano and M. Fumoto of Tokyo Institute of Technology for experimental assistance and use of equipment in several phases of the investigation.

The author expresses thanks to H. Yamamura of Osaka University and Dr. M. Yoshimura of Tokyo Institute of Technology for communicating opinions on related topics, and also to K. Murata of

Osaka University for some advices in chemical analysis.

The author wish to gratefully acknowledge many helpful comments with a number of colleagues of Osaka University and Tokyo Institute of Technology.

The author also wish to express his gratitude to Miss Y. Hirasaki of Tokyo Institute of Technology for her typing the manuscripts.

References

1) R. Scholder, F. Kindervater, and W. Zeiss, "Über Metaferrate (IV)", Z. anorg. allgem. Chem., 283, 338-345 (1956).

2) M. Erchak, Jr., I. Fankuchen and R. Ward, "Reaction between Ferric Oxide and Barium Carbonate in the Solid Phase Identification of Phases by X-ray Diffraction", J. Am. Chem. Soc., 68, 2085-2093 (1946).

3) J. B. MacChesney, R. C. Sherwood, and J. F. Potter,"Electric and Magnetic Properties of the Strontium Ferrates", J. Chem. Phys., 43, 1907-1913 (1965).

4) H. J. Van Hook, "Oxygen Stoichiometry in the Compound $BaFeO_{3-x}$", J. Phys. Chem., 68, 3786-3789 (1964).

5) J. B. MacChesney, J. F. Potter, R. C. Sherwood, and H. J. Williams, "Oxygen Stoichiometry in the Barium Ferrates; Its Effect on Magnetization", J. Chem. Phys., 43, 3317-3322 (1965).

6) S. Mori, "Magnetic Properties of Several Phases of Barium Orthoferrate, $BaFeO_x$", J. Phys. Soc. Japan, 28, 44-50 (1970).

7) M. B. Robin and P. Day, "Mixed Valence Chemistry-A Survey and Classification", Advances in Inorganic Chemistry and Radiochemistry (edited by H. J. Emeleus and A. G. Sharpe), Academic Press, New York, 10, 247-422 (1967).

8) H. Watanabe, "Magnetic Properties of Perovskites Containing Strontium: I. Strontium-Rich Ferrites and Cobaltites", J. Phys. Soc. Japan, 12, 515-522 (1957).

9) T. R. Clevenger, Jr., "Effect of Fe^{4+} in the System $SrFeO_3$-$SrTiO_3$", J. Am. Cer. Soc., 46, 207-210 (1963).

10) P. K. Gallagher, J. B. MacChesney, and D. N. E. Buchanan, "Mössbauer Effect in the System $SrFeO_{2.5-3.0}$", J. Chem. Phys., 41, 2429-2434 (1964).

11) U. Shimony, and J. M. Knudsen, "Mössbauer Studies on Iron in the Perovskites $La_{1-x}Sr_xFeO_3(0 \leq x \leq 1)$", Phys. Rev., 144, 361-356 (1966).

12) J. B. MacChesney, J. J. Jetzt, J. F. Potter, H. J. Williams, and R. C. Sherwood, "Electrical and Magnetic Properties of the System $SrFeO_3$-$BiFeO_3$", J. Am. Cer. Soc., 49, 644-647 (1966).

13) P. K. Gallagher, J. B. MacChesney, and D. N. E. Buchanan, "Mössbauer Effect in the System $BaFeO_{2.5-3.0}$", J. Chem. Phys., 43, 516-520 (1965).

14) a) N. Mizutani, A. Kitazawa, N. Ohkuma, and M. Kato, "Synthesis of Strontium-Manganese Double Oxides", Kogyo Kagaku Zasshi, 73, 1097-1103 (1970). [in Japanese].

b) N. Mizutani, N. Ohkuma, A. Kitazawa, and M. Kato, "Modification and Oxygen Deficiency of Strontium-Manganese Double Oxides, $SrMnO_{3-\delta}(\delta = 0-0.5)$", Kogyo Kagaku Zasshi, 73, 1103-1110 (1970). [in Japanese].

15) A. F. Wells, "Structural Inorganic Chemistry", Oxford Univ. Press (3rd ed.), 494-499 (1967).

16) E. F. Bertaut, P. Blum, and A. Sagnieres, "Structure du Ferrite Bicalcique et de la Brownmillerite", Acta Cryst., 12, 149-159 (1959).

17) A. A. Colville, "The Crystal Structure of $Ca_2Fe_2O_5$ and its Relation to the Nuclear Electric Field Gradient at the Iron Sites", Acta Cryst., B26, 1469-1473 (1970).

18) I. M. Kolthoff and E. B. Sandell, "Textbook of Quantitative Inorganic Analysis", Macmillan Comp. (3rd ed.), New York, 564-578 (1952).

19) J. J. Spijkerman, F. C. Ruegg, and J. R. Devoe, "Standardization of the Differential Chemical Shift for Fe^{57}", Mössbauer Effect Methodology (edited by I. J. Gruverman), Plenum Press, New York, 1, 115-120 (1965).

20) K. Ono, and A. Ito, "A Mössbauer Study of the Internal Field at Fe^{57} in α-Fe_2O_3", J. Phys. Soc. Japan, 17, 1012-1017 (1962).

21) R. S. Preston, S. S. Hanna, and J. Heberle, "Mössbauer Effect in Metallic Iron", Phys. Rev., 128, 2207-2218 (1962).

22) J. Reekie, "The Magnetic Susceptibilities of some Cupric Salts", Proc. Poy. Soc. (London), A, 173, 367-378 (1939).

23) N. Nagasako, K. Sato, and R. Kiyoura, "Kogyo-Kagaku-Keisan (Calculus on Industrial Chemistry)", Hirokawa Publishing Co., Tokyo, 168 (1969). [in Japanese].

24) G. Shirane and D. E. Cox, "Mössbauer Study of Isomer Shift, Quadrupole Interaction, and Hyperfine Field in several Oxides Containing Fe^{57}", Phys. Rev., 125, 1158-1165 (1962).

25) S. Geller, R. W. Grant, U. Gonser, H. Wiedersich, and G. P. Espinosa, "Intrasublattice Antiferromagnetism in $Ca_2[Fe](Fe)O_5$", Phys. Letters, 20, 115-117 (1966).

26) F. Wittmann and F. Pobell, "Messungen an Fe^{57} in Calcium-aluminatferriten mit Hilfe des Mößbauer-Effekts", Z. Naturforschg. 21a, 831-835 (1966).

27) U. Gonser, R. W. Grant, H. Wiedersich, and S. Geller, "Spin Orientation Determination by Linearly Polarized, Recoil-Free γ Rays (Mössbauer effect; antiferromagnetic $Ca_2[Fe](Fe)O_5$; E/T)", Appl. Phys. Letters, 9, 18-21 (1966).

28) R. W. Grant, "Nuclear Electric Field Gradient at the Iron Sites in $Ca_2Fe_2O_5$ and Ca_2FeAlO_5", J. Chem. Phys., 51, 1156-1162 (1969).

29) G. H. Jonker and J. H. van Santen, "Ferromagnetic Compounds of Manganese with Perovskite Structure", Physica, 16, 337-349 (1950).

30) J. B. Goodenough, "Theory of the Role of Covalence in the Perovskite-Type Manganites [La, M(II)]MnO_3", Phys. Rev., 100, 564-573 (1955).

31) E. O. Wollan and W. C. Koehler, "Neutron Diffraction Study of the Magnetic Properties of the Series of Perovskite-Type Compounds [(1-x)La, xCa]MnO_3", Phys. Rev., 100, 545-563 (1955).

32) G. H. Jonker, "Magnetic Compounds with Perovskite Structure IV: Conducting and Non-conducting Compounds", Physica, 22, 707-722 (1956).

33) A. D. Wadsley, "Inorganic Non-Stoichiometric Compounds", Non-Stoichiometric Compounds (edited by L. Mandelcorn), Academic Press, New York and London, 134-136 (1964).

34) V. M. Goldschmidt, "Geochemische Verteilungsgesetze der Elemente", Skrifter Norske Videnskaps-Akad. Mat. Naturvid. Kl. No. 8 (1926).

35) H. L. Yakel, "On the Structures of some Compounds of the Perovskite Type", Acta Cryst., 8, 394-398 (1955).

36) H. D. Megaw, "Crystal Structure of Double Oxides of the Perovskite Type", Proc. Phys. Soc. Part 2, 58, 133-152 (1946).

37) M. L. Keith and R. Roy, "Structural Relations among Double Oxides of Trivalent Elements", Am. Mineral., 39, 1-23 (1954).

38) R. S. Roth, "Classification of Perovskite and Other ABO_3-Type Compounds", J. Res. N. B. S., 58, 75-88 (1957).

39) R. Kiriyama and H. Kiriyama, "Kozo-Muki-Kagaku (Structural Inorganic Chemistry)", Kyoritsu Shuppan, Tokyo, I, 282 (1964).

40) L. R. Walker, G. K. Wertheim, and V. Jaccarino, "Interpretation of the Fe^{57} Isomer Shift", Phys. Rev. Letters, 6, 98-101 (1961).

41) G. K. Wertheim and R. H. Herber, "Resonant Gamma-Ray Absorption in Potassium Ferrate", J. Chem. Phys., 36, 2497-2499 (1962).

42) P. K. Gallagher, J. B. MacChesney, and D. N. E. Buchanan, "Mössbauer Effect in the System $Sr_3Fe_2O_{6-7}$", J. Chem. Phys., 45, 2466-2471 (1966).

43) J. H. de Boer and E. J. W. Verwey, "Semi-Conductors with Completely Filled 3d-Lattice Bands", Proc. Phys. Soc. (London), 49, 59-71 (1937).

44) J. B. Goodenough, "Covalency Criterion for Localized vs. Collective Electrons in Oxides with the Perovskite Structure", J. Appl. Phys., 37, 1415-1422 (1966).

46) J. B. Goodenough and P. M. Raccah, "Complex vs. Band Formation in Perovskite Oxides", J. Appl. Phys. Suppl., 36, 1031-1032 (1965).

45) B. L. Chamberland, "Preparation and Properties of $SrCrO_3$", Solid State Communications, 5, 663-666 (1967).

47) B. Kubota, "Decomposition of Higher Oxides of Chromium Under Various Pressures of Oxygen", J. Am. Cer. Soc., 44, 239-248 (1961).

48) R. Roy, "Controlled pO_2 Including High Oxygen Pressure Studies in Several Transition Metal-Oxygen Systems", Bull. Soc. chim. France, 1965, 1065-1069 (1965).

49) O. Fukunaga and S. Saito, "Phase Equilibrium in the System CrO_2-CrO_3", J. Am. Cer. Soc., 51, 362-363 (1968).

50) R. C. DeVries, "Stability of CrO_2 at High Pressures and Temperatures in the 'Belt' Apparatus", Mater. Res. Bull., 2, 999-1007 (1967).

51) I. M. Kolthoff and P. J. Elving, "Treatise on Analytical Chemistry", Part II, Interscience, 5, 129 (1961).

52) J. Kashima, "Chromium in Steel (Colorimetry)", Jikken-Kagaku-Koza (Experimental Chemistry Course), Maruzen, Tokyo, 15, 193-194 (1958). in Japanese .

53) R. W. Kiser, "Tables of Ionization Potentials", U. S. Atomic Energy Comission TID 6142 (1960).

Appendix

Ionization potentials of 3d-elements[53] are presented in Fig. A1. The fourth ionization energy of iron is 1310 kcal/mole, whereas the third one is 706.7 kcal/mole. Therefore, it requires 603.3 kcal in order to obtain one molecule of $AFeO_3$(IV) with the perovskite structure by the oxidation of a half mole of $Ca_2Fe_2O_5$ (III) with the brownmillerite-like structure via the transition from Fe^{3+} to Fe^{4+}.

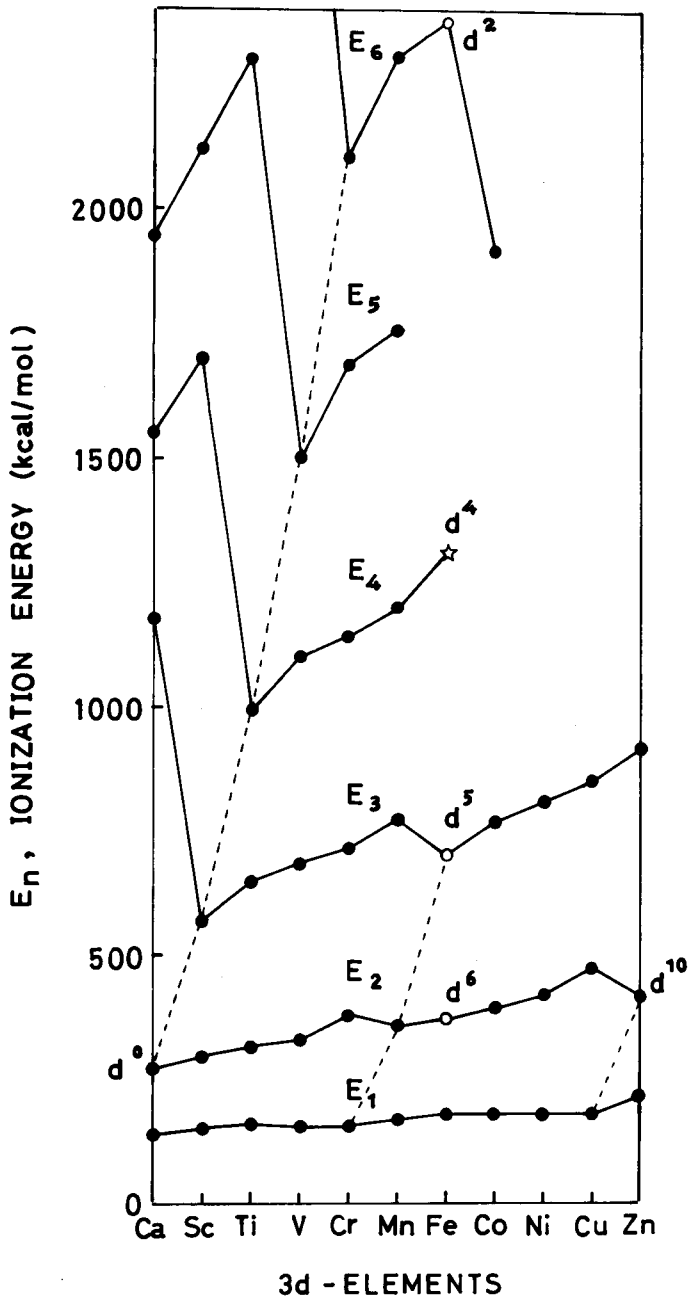

Fig. A1. Ionization energy for 3d-elements.